Taylor & Francis
Taylor & Francis Group

REVIEW ARTICLE

🔓 OPEN ACCESS ⓤ Check for updates

Distinctive characteristics of carrier-phonon interactions in optically driven semiconductor quantum dots

D. E. Reiter [iD][a], T. Kuhn [iD][a] and V. M. Axt[b]

[a]Institut für Festkörpertheorie and Center for Multiscale Theory and Computation (CMTC), Universität Münster, Münster, Germany; [b]Theoretische Physik III, Universität Bayreuth, Bayreuth, Germany

ABSTRACT

We review distinct features arising from the unique nature of the carrier-phonon coupling in self-assembled semiconductor quantum dots. Because of the discrete electronic energy structure, the pure dephasing coupling usually dominates the phonon effects, of which two properties are of key importance: The resonant nature of the dot-phonon coupling, i.e. its non-monotonic behavior as a function of energy, and the fact that it is of super-Ohmic type. Phonons do not only act destructively in quantum dots by introducing dephasing, they also offer new opportunities, e.g. in state preparation protocols. Apart from being an interesting model systems for studying fundamental physical aspects, quantum dot and quantum dot-microcavity systems are a hotspot for many innovative applications. We discuss recent developments related to the decisive impact of phonons on key figures of merit of photonic devices like single or entangled photon sources under aspects like indistinguishability, purity and brightness. All in all it follows that understanding and controlling the carrier-phonon interaction in semiconductor quantum dots is vital for their usage in quantum information technology.
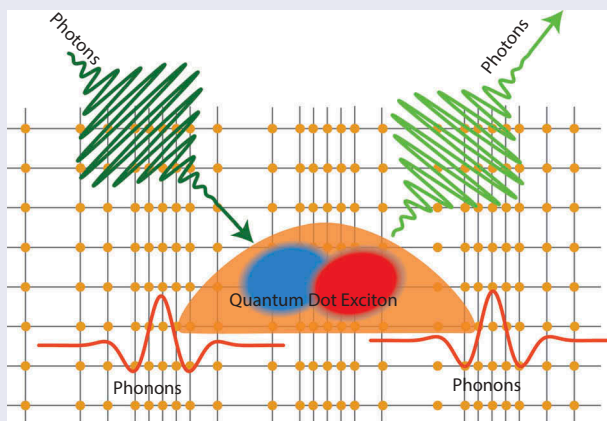
CONTACT D. E. Reiter ✉ Doris.Reiter@uni-muenster.de 🖵 Institut für Festkörpertheorie and Center for Multiscale Theory and Computation (CMTC), Universität Münster, Münster, Germany

1. Introduction

When solids are reduced to the nano-scale, several properties of the system become fundamentally different than on the macro-scale. Most obviously, this holds for the electronic energy structure. A semiconductor quantum dot (QD) is a nano-structure, where a material with a low band gap is embedded into a material with a higher band gap yielding a three dimensional confinement of the carriers and, thus, a discrete energy structure [1–5]. Due to the discrete energies QDs are often referred to as *artificial atoms*. Unlike real atoms, the energies of QDs can be tailored in a wide range by changing their size and geometry [6] making them attractive for many applications. An equally important difference to atomic systems is the fact that QDs are embedded in a solid state environment. In particular, the coupling to the motion of lattice atoms, that after quantization gives rise to quasi-particles denoted as *phonons*, has a profound impact on the physics of QD systems.

In this review, we highlight the distinctive characteristics of the QD-phonon interaction which differs significantly from carrier-phonon interactions in extended semiconductors. In fact, in bulk materials or in two-dimensional semiconductors, like the recently found monolayers of transition metal dichalcogenides [7,8], there are usually many possibilities to reach another electric state from a given initial state by a phonon emission or absorption process that respects the conservation of energy and momentum on the single particle level. However, phonon energies do typically not match the discrete electronic transition energies in QDs. This mismatch of transition energies was expected to result in a hindrance of relaxation in QDs, which was coined by the term *phonon bottleneck* [5,9–12]. Due to the phonon bottleneck, the phonon-induced coupling between different electronic states can be rather weak in QDs and a different carrier-phonon coupling mechanism becomes dominant, at least on short time scales on the order of a few to tens of picoseconds, namely, *pure dephasing* processes due to acoustic phonons [13,14]. Here, the phonons couple to the occupations of QD states rather than to transitions between different states. As a consequence, in the free time evolution that arises, e.g. after an excitation of a QD with an ultra-fast laser pulse, such a QD-phonon coupling can affect only the electronic coherences while the occupations are conserved. However, it should be noted that, as a result of further interactions, like, e.g. permanent laser driving or the coupling to photon modes of a cavity, new electronic states emerge such as laser or cavity-dressed states. While pure dephasing interactions are unable to induce transitions between the undressed states, they can lead to relaxations between the dressed states. Examples where such relaxation processes become important are the phonon induced damping of Rabi oscillations [15–21], the phonon influence on state preparation schemes [22–27] or phonon-assisted cavity feeding [28–37]. We will discuss these and other effects in our review and show that all of them reflect distinctive features

of the carrier-phonon interaction, examples being a non-resonant coupling enabled by phonons, asymmetries in the coupling efficiency and non-Markovian characteristics.

Longitudinal optical (LO) phonons on the other hand can provide efficient relaxation channels between excited QD states, especially via multi-phonon transitions [38–41]. An exceptional situation is encountered when LO phonons happen to have energies close to resonance with transitions between different discrete excited states of a QD. In this case, a strong QD-phonon coupling regime with clear anti-crossing behavior is encountered indicating the emergence of a new quasi-particle. Due to its exceptional stability it is termed *everlasting resonant polaron* [42,43]. Further analysis revealed that the polaron lifetime is mainly limited by the decay of the LO-phonon component via anharmonic phonon-couplings into two other phonons, where different branches (acoustic or optical) are possible for the final phonons [44–47].

While QDs are interesting objects for studying the fundamentals of the carrier-phonon interaction on the nano-scale, they are likewise highly attractive candidates for applications in quantum information technology. In particular, QDs could be used as single [48–55] or pair photon sources [54,56–63] or in quantum networks [64]. Therefore it is also of high interest to understand the impact of the carrier-phonon interaction on the properties of the photons emitted from a QD.

The remainder of the paper is organized as follows: We start by briefly summarizing the basics of the theoretical description of the carrier-phonon interaction in QDs (Sec. 2) including a discussion of commonly used approaches to simulate observable quantities (Sec. 2.3). We then review a few instructive examples of the phonon impact on linear and non-linear optical signals (Sec. 3) and present theoretical and experimental results highlighting the resonant nature of the carrier-phonon coupling (Sec. 4). The distinctive influence of phonons on photonic properties is addressed in Sec. 5 and we conclude in Sec. 6 with some outlook towards future research.

2. Modelling of the carrier-phonon interaction in quantum dots

2.1. Electronic structure

Due to its discrete energy structure, the electronic degrees of freedom of a QD can be well approximated by a few-level system as long as the remaining states are not excited. In a neutral QD, the simplest few-level system is composed of the ground state $|g\rangle$ at the energy $\hbar\omega_g$, where no excitation took place, and the lowest excited state $|x\rangle$ consisting of one exciton (electron-hole pair) at the energy $\hbar\omega_x$. When the QD is exposed to laser driving or is embedded in a cavity, these two states are coupled by the

dipole interaction between the electric field **E** and the QD polarization **P**. In the two-level approximation the Hamiltonian of the system can be written as

$$H_{\text{QD}} = \hbar\omega_g |g\rangle\langle g| + \hbar\omega_x |x\rangle\langle x| - \mathbf{P} \cdot \mathbf{E}. \qquad (1)$$

Despite its simplicity the two-level model already captures many of the pertinent physical aspects that are also found in more involved situations. Therefore, it is often the starting point for the analysis. Since the two-level model implicitly assumes a selective coupling where the frequencies of the electric field are nearly resonant to the QD transition frequency, it is common to apply the rotating wave approximation to the dipole coupling [65]. The electric field can be modeled either by a classical light field or by quantized photon modes. The former is a valid description when the QD is driven by a coherent external laser; a situation encountered, e.g. in state preparation schemes or when measuring absorption spectra. The latter results in the Jaynes-Cummings model known from quantum optics [66–68]. This level of theory is required when considering a QD in a cavity or when studying photonic properties like the indistinguishability of emitted photons. Often a diagonalization of the coupled electronic-light Hamiltonian is advantageous for the interpretation which introduces the dressed state basis [24], that is, however, time-dependent for pulsed excitation.

A more complete description of a QD has to account for several excitonic states. Restricting ourselves to the excitation of s-shell excitons, there are four different configurations of electron and hole spin. From these four single exciton states two are optically active or bright, while the other two are optically inactive or dark and, thus, other than optical means are needed for addressing the latter states [69–71]. In the s-shell manifold also the excitation of two excitons is possible resulting in the biexciton state, which is used as the starting point for entangled photon-pair generation. A more detailed discussion of the states and their optical selection rules can be found, e.g. in Refs [2,5,24,72]. For small QDs, which are in the strong confinement limit, the restriction to s-shell excitons holds rather well. For larger QDs or higher shells, state mixing effects can become important leading to modified selection rules [73].

2.2. Carrier-phonon interaction

Accounting for single exciton and biexciton states in addition to the QD ground state, the Hamiltonian of the phononic part and the QD-phonon interaction for a strongly confined QD can be written as

$$H_{\text{ph}} = \hbar \sum_{\mathbf{q}} \omega_{\mathbf{q}} b_{\mathbf{q}}^{\dagger} b_{\mathbf{q}} + \hbar \sum_{\mathbf{q},\chi} n_{\chi} |\chi\rangle\langle\chi| \left(g_{\mathbf{q}} b_{\mathbf{q}} + g_{\mathbf{q}}^{*} b_{\mathbf{q}}^{\dagger} \right), \qquad (2)$$

where $b_{\mathbf{q}}^{\dagger} (b_{\mathbf{q}})$ are the creation (annihilation) operators of a phonon with wave vector $\mathbf{q}$ having the energy $\hbar\omega_{\mathbf{q}}$ and χ labels the QD states, where n_{χ} denotes the number of electron-hole pairs contained in a state $|\chi\rangle$. The carrier-phonon coupling is given by the coupling matrix element $g_{\mathbf{q}}$. The fact, that the phonon-coupling is determined for all states $|\chi\rangle$ by the same function $g_{\mathbf{q}}$ just scaled by the number of pairs n_{χ} is a consequence of considering the strong confinement limit where exciton and biexciton wave functions factorize into products of single-particle wave functions. Further, we point out that the pure dephasing nature of this coupling mechanism manifests itself in the coupling term being proportional to $|\chi\rangle\langle\chi|$ and not to transitions between states.

There are several mechanisms of carrier-phonon interaction, among them the deformation potential coupling, the piezoelectric coupling and the Fröhlich coupling. For the dephasing, that constitutes the most important phonon impact on short time scales, usually the deformation potential coupling to longitudinal acoustic (LA) phonons dominates [14,15,24,74,75]. Exceptions to this rule occur in particular for GaN-based QDs [76,77] where the piezoelectric coupling to both longitudinal and transverse acoustic phonons can become comparable or even stronger than the deformation potential coupling due to the huge internal fields that build up in these structures. The Fröhlich coupling is the main interaction mechanism for LO phonons which, however, do not contribute much to the dephasing [14]. This is due to their weak dispersion as well as to the fact that LO phonons introduce only fast oscillating off-resonant contributions to the dynamics; except for special cases where LO phonon energies happen to be close to transition energies to higher electronic states. For QD states close to the wetting layer LO phonons may also contribute when additionally carrier-carrier scattering comes into play [78,79]. We further emphasize, that the Fröhlich interaction strength depends on the difference between electron and hole wave function [14]. This difference is rather weak in standard GaAs-type QDs, hence the influence of LO phonons in these dots is negligible, while for type-II QDs [80] or a QD in an electric field [76] the LO phonon coupling can become strong [81].

In this review we concentrate on materials with similar lattice properties for the QD and its surrounding, which applies, in particular, to the widely studied class of InGaAs/GaAs-type QDs. A cross section of an InGaAs QD obtained by transmission electronic microscopy (TEM) is shown in Figure 1 (left) displaying the typical lens-shape of a self-assembled QD. The scale bar gives the size of the QD with its borders being at a radius of about 10-20 nm in in-plane direction and a height of 3-7 nm. Note that the size of the QD in the remainder of this review refers of the width of the
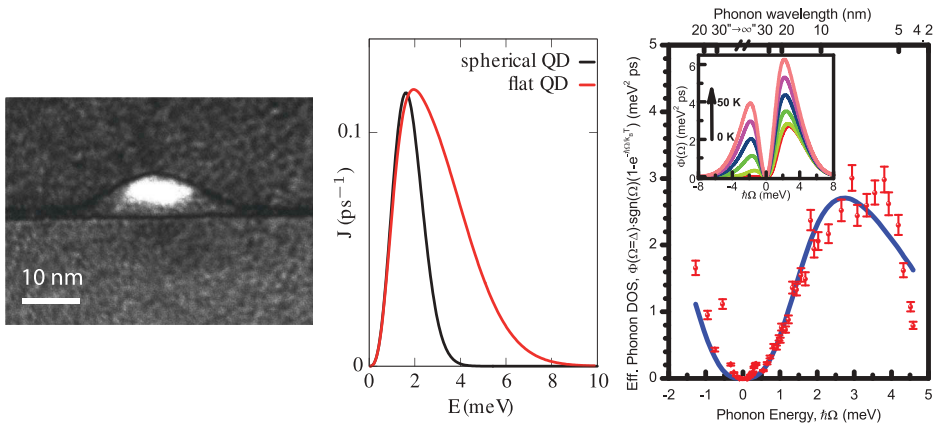
Figure 1. Left: Transmission electron microscopy (TEM) picture of a cross section of a single InGaAs QD. Figure by A. Ludwig and J-M. Chauveau [94]© Nature Publishing Group. Center: Calculated phonon spectral density for a spherical QD with a size of 3.8 nm and a flat QD with a lateral size of 5 nm and a height of 1.5 nm. Right: Measured effective phonon spectral density (dots) fitted by a theoretical calculation. The measurements were taken at $T = 10$ K. The inset shows the calculated effective phonon spectral density for different temperatures. The right part is taken from [100]© American Physical Society.

envelope carrier wave functions in the QD, which is typically smaller by about one half.

For such QDs the phonons are almost not affected by the QD confinement and can be well described as bulk phonons, i.e. plane wave eigenmodes that have well defined momenta **q** and corresponding energies $\hbar\omega_{\mathbf{q}}$. Note that this is different especially for QDs surrounded by a glass matrix [82–87] or colloidal QDs [88–91], which are often dissolved in liquids and have a strong dependence of the phonon dispersion on the size and shape of the dot, or for metallic nano-particles which show vibrational modes of the whole particle [92].

For bulk phonons, the coupling matrix element $g_{\mathbf{q}} = \mathcal{G}_{\mathbf{q}}\mathcal{F}_{\mathbf{q}}$ factorizes into the bulk matrix element $\mathcal{G}_{\mathbf{q}}$ and a form factor $\mathcal{F}_{\mathbf{q}}$, which can be calculated within the envelope function formalism from the QD wave function via a Fourier transform. Due to the form factor, the coupling is restricted to low q-values, where the dispersion of acoustic phonons can be approximated by a linear function $\omega_{\mathbf{q}} = c_s q$ with c_s being the speed of sound. The explicit form of the coupling matrix elements for different mechanisms can be found, e.g. in Refs [14,24,76,93].

The coupling efficiency can be well illustrated using the phonon spectral density defined as $J(\omega) = \sum_{\mathbf{q}} |g_{\mathbf{q}}|^2 \delta(\omega - \omega_{\mathbf{q}})$. Examples of calculated and measured phonon spectral densities are shown in Figure 1. The most remarkable feature of $J(\omega)$ is its non-monotonic dependence on energy such that a maximum is found at a finite energy. This maximum is the

origin of the resonant nature of the QD phonon coupling. Resonant in this case means that when the light-dressed states have a splitting corresponding to this maximum the electron-phonon coupling has its highest efficiency.

We will see and discuss consequences of this non-monotonic behavior further in Sec. 4. The appearance of the maximum can be understood in view of the decomposition of the phonon coupling into a bulk matrix element and a form factor: While for small energies the bulk coupling matrix element dominates and exhibits for deformation potential coupling a cubic behavior $\sim \omega^3$, at high energies the phonon spectral density is determined by the form factor, which rapidly approaches zero. As a side-aspect we note that, depending on the parameters, the spectral density can also have a zero at finite energies [95].

The specific shape of the phonon spectral density depends sensitively on the actual size of the QD. For a spherical QD [black curve in Figure 1 (center)], the phonon spectral density can be well approximated by $J(\omega) \sim \omega^3 \exp(-\omega^2/\omega_c^2)$ with the cut-off frequency ω_c [96]. Typical QDs are lens-shaped rather than spherical [red curve in Figure 1 (center)]. The phonon spectral density for the flat QD has a larger ω-extension than found for the spherical QD in Figure 1 because its smallest spatial confinement corresponding to its height is smaller than the QD radius in the spherical case and thus phonons with higher energies are coupled. It should be noted, however, that since $J(\omega)$ is a single function of a single real parameter, for any given $J(\omega)$ (no matter whether it has been calculated for a spherical or a non-spherical QD) it is always possible to find a spherical QD model that yields the same phonon spectral density [93]. This is an important observation since from the formal representation of the dynamics within the path-integral formalism [97] it is readily seen that all phonon influences on the dynamics of the reduced electronic density matrix for a strongly confined system are mediated by $J(\omega)$. Therefore, the electronic dynamics can always be treated in a spherical QD model without loss of generality. The phonon degrees of freedom, on the other hand, reflect the QD shape and geometry as well as anisotropies of the QD-phonon coupling as can be seen, e.g. from the spatio-temporal evolution of phonon wave packets emitted from QDs [76,98,99].

Figure 1 (right) displays a measured effective phonon spectral density defined as $J^{\text{eff}}(\omega) = \sum_{\mathbf{q}} |g_{\mathbf{q}}|^2 [n_{\mathbf{q}}(T)\delta(\omega + \omega_q) + (n_{\mathbf{q}}(T) + 1)\delta(\omega - \omega_q)]$, where the occupation of the phonons is taken into account explicitly by the Bose distribution $n_{\mathbf{q}}(T)$ [100]. The measurement was performed for a QD embedded in a photonic crystal cavity, where the phonon spectral density was extracted by quantifying the phonon-assisted cavity feeding [100]. The inset in Figure 1 (right) displays calculated $J^{\text{eff}}(\omega)$ curves for different temperatures, which agree well with the measurements. Again we

see the finite range of the phonon spectral density and its resonant nature. Since the effective phonon spectral density takes into account the temperature, it reveals the asymmetry between emission and absorption of the phonons. At low temperatures, the phonon occupations are negligible and, hence, there are no phonons that could be absorbed. Therefore, only phonon emission processes take place. Accordingly the effective phonon spectral density is only non-vanishing for $\omega_q > 0$. With increasing temperature phonon absorption becomes possible and J^{eff} becomes more and more symmetric.

2.3. Theoretical approaches

When there is no light-field acting on the system, the QD model introduced in the previous subsections reduces to the *independent boson model*, for which analytical solutions exist [101–104]. However, as soon as a light field is active, in the most general case no analytical solution is known and approximate or numerical solutions to the coupled QD-light-phonon problem are employed. Because of their importance for the theory of quantum dissipative systems in general and their relative simplicity, models of the here discussed type have become a test-field for approximate approaches and the development of new methods. Indeed, almost any many-body technique has been applied in order to evaluate the dynamics predicted by these models.

In the case of ultra-fast optical excitation, i.e. when the laser pulses can be approximated by δ-pulses, analytical solutions of the problem can be found by separating the light field and phonon induced dynamics and employing a generating function formalism [105–107]. The analytic solution accounts for both the electronic and phononic degrees of freedom and also allows to study phonon properties like, e.g. the lattice displacement field and its fluctuations, which under certain circumstance exhibit phonon-squeezing [81,108,109]. Furthermore, linear and non-linear optical signals can be obtained exactly [14,74,110–112]. Recently, analytical results for the absorption spectrum have been obtained for a two-level system coupled to a single phonon mode even including quadratic QD-phonon couplings [113].

A popular method for obtaining numerical solutions is provided by the correlation (or cluster) expansion within the density matrix formalism [15,17,93,114–119]. Here, equations of motion for variables of interest are set up, but, due to the many-body character of the carrier-phonon interaction, they are not closed since higher order terms appear (i.e. expectation values of a larger number of operators for electronic, photonic or phononic degrees of freedom). The higher order terms are factorized into cumulants [120] and the correlated parts are used as new dynamic variables, which yields an infinite hierarchy of coupled equations for correlation functions.

To truncate these equations, higher order correlations are neglected at some order. Typically, a rather high accuracy is obtained within the fourth order Born approximation [116]. The corresponding equations of motion can be found e.g. in Ref [114]. The approach has been generalized by introducing a photon-probability cluster expansion to take into account a quantized light field [115]. A further advantage of the correlation expansion is that it explicitly takes into account the phonon degrees of freedom and thus provides directly information about the phonon dynamics [93,118].

The master equation approach is a standard workhorse for treating quantum dissipative systems [121,122]. Master equations have been derived for the systems considered in this review on different levels of complexity [20,123–129]. One approach, which lately has attracted much attention, is the polaron master equation (PME) [130–132]. In the PME treatment the coupled QD-light field and the polaron contribution of the carrier-phonon interaction are taken as system, while the dissipative part of the carrier-phonon interaction constitutes the bath. The latter is usually treated perturbatively. The second order Born-Markov approximation of the QD-phonon coupling (also known as *weak-coupling theory*) yields at higher temperatures unphysical negative values for the exciton occupations [123,132]. This can be overcome by switching to a polaron-transformed frame [123,132]. The transformation to the polaron frame need not necessarily be complete but can be controlled by a variational parameter [20]. A review on the PME approach can be found in Ref [132]. Recently, an extension to the standard PME has been developped to improve the accuracy of the method for systems exposed to a time-dependent drive [133]. Another variant of the master equation approach is the time-convolutionless (TCL) projection operator method [121] which has also been applied successfully to describe effects of the carrier-phonon coupling in QDs [134–139].

Other many-particle techniques that have been applied to the dynamics and relaxation of QDs coupled to phonons cover Green-functions [140–143], multi-configuration time-dependent Hartree methods [142], time-dependent density functional theory [90,144] as well as path-integrals (PI) [97,145,146]. In particular, real-time PI methods have been widely used [21,147–157]. With these methods it is possible to evaluate the reduced electronic density matrix for QD-phonon systems without approximation to the model. Interestingly, the PI method performs even better for strong couplings, where perturbative methods come to their limits [151]. Most of the current calculations rely on the pioneering work of Makri and Makarov [145,146], where, starting from Feynman's exact representation of the time-evolution operator in Hilbert space [158,159], an iteration scheme for the so called augmented density matrix (ADM) was introduced that exploits the finite extension of the phonon induced memory. It turns out, that these ideas can be extended to Liouville space [156] which allows the natural inclusion of non-Hamiltonian

contributions to the dynamics like, e.g. Lindblad-type loss-rates, along with the numerically complete treatment of QD-phonon couplings. Due to the rapid increase of the numerical demand with the number of system states, PI based simulations of the QD-phonon dynamics have for a long time been restricted to systems with at most four states. Recently, however, a laser driven QD-cavity system with 41 states coupled to a continuum of LA phonons has been treated in a numerically complete way [37]. This became possible due to a reformulation of the iteration scheme where now a partially summed ADM is iterated which in the case considered in Ref [37] reduced the number of variables that need to be iterated by more than 15 orders of magnitude. The efficiency of PI calculations can be further boosted by using tensor-network techniques [157]. PI methods have also been developed for the evaluation of multi-time correlation functions [160]. This paves the way for overcoming limitations of the widely used quantum regression theorem resulting from the fact that this theorem is valid only when all baths introduce a Markovian-type dynamics [122,161,162].

3. Phonon impact on optical signals

3.1. Linear optical response

The influence of the carrier-phonon interaction is already clearly visible in the linear absorption or emission spectra of a QD [13,14]. Due to the discrete energy structure of the QD levels, one would expect to see a sharp transition line corresponding to the transition energy between the states. This line is referred to as *zero phonon line* (ZPL). The ZPL is superimposed on a broad phononic background. An example of a calculated emission spectrum is shown in Figure 2 (left) taken from Ref [163]. At low temperatures, the phonon background is visible only at one side of the ZPL, reflecting the difference in emission and absorption. At higher temperatures, it becomes more symmetric as phonon emission and absorption processes become more balanced. The phonon background reflects the phonon spectral density (cf. Figure 1) and has an energy range of a few tens of meV. Absorption spectra exhibit analogous features [14].

The phonon sidebands in the photoluminescence spectrum of a single QD have been measured more than 15 years ago [13] and have been confirmed several times since then [164–167]. More recently, QDs have been embedded into photonic cavities [53,163,168,169], which have a line-width smaller than the width of the phonon background. Figure 2 (right) displays the spectrum of a QD within a cavity (red line) and without a cavity (black line) [168]. Embedding the QD in a cavity has two essential effects: the ZPL is broadened due to the Purcell enhancement of the radiative emission and the phonon sideband emission falling outside the spectrum of the empty

cavity (blue dashed line) is strongly suppressed. Thus, the cavity effectively redirects the phonon sideband emission towards the ZPL.

The spectral information can be connected to the temporal behavior of the linear polarization induced by an ultra-short laser pulse [14]. In the dynamics of the polarization, a sharp drop within the first few picoseconds is followed by a long-term decay on a nanosecond time-scale. The initial loss of coherence is due to the acoustic phonons that are also responsible for the phonon sidebands. It can be noticeably reduced by using a multi-pulse coherent control scheme [170]. After excitation with a single short pulse, the asymptotic of the polarization obtained for long times when only pure dephasing type couplings to acoustic phonons are retained is exclusively governed by the behavior of the dimensionless QD-phonon coupling $\gamma_{\mathbf{q}} = \frac{g_{\mathbf{q}}}{\omega_{\mathbf{q}}}$ in the limit of small q values (cf. the appendix of Ref [14]). It is important to note, that $g_{\mathbf{q}}$ is the difference between the phonon couplings to electrons and holes. For piezoelectric coupling cancellations caused by taking the difference lead to a different small q scaling of $g_{\mathbf{q}}$ than that obtained individually for the electron and hole couplings [14]. For phonons with linear dispersion $\omega_{\mathbf{q}} = c_s q$ a small q asymptotic of $|\gamma_{\mathbf{q}}|^2 \sim q^\lambda$ directly translates into a power law $J(\omega) \sim \omega^n$ with $n = \lambda + 4$ for the phonon spectral density. At finite temperatures, an exponential decay of the polarization is obtained for $n = 1$, which is referred as the Ohmic case [121]. For sub-Ohmic coupling ($n < 1$) the decay can be even stronger. Deformation potential coupling yields $n = 3$ while $n = 5$ is obtained for piezoelectric interactions (i.e. super-Ohmic couplings in both cases) indicating that
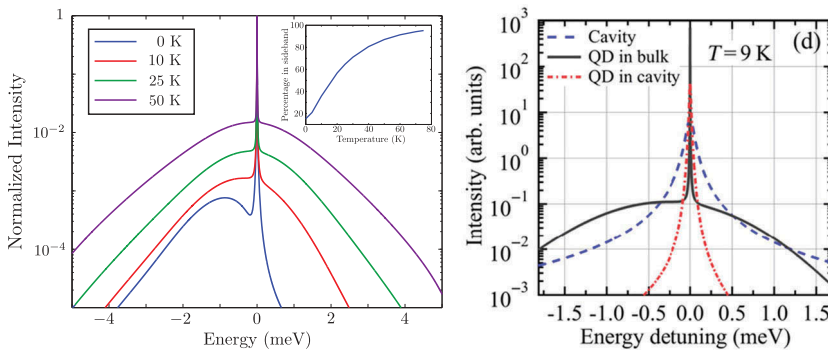
Figure 2. Left: Calculated normalized emission spectrum from a single QD at different temperatures. Note the logarithmic scale. Inset: fraction of the intensity in the sidebands. Taken from Ref [163].© American Physical Society. Right: Calculated spectrum from a QD in a photonic cavity (red dotted line) and without cavity (black line). The cavity spectrum is indicated by the blue, dashed line. Note the logarithmic scale. Taken from Ref [168].© American Physical Society.

the polarization decays non-exponentially towards a finite value at long times. This implies that the pure dephasing model for acoustic phonons provides no contribution to the width of the ZPL.

At low temperatures the ZPL acquires a finite width due to the radiative decay of the exciton which for a QD takes place on a nanosecond timescale, i.e. much longer than typical phonon induced time scales [13,171,172]. Furthermore a noticeable temperature dependence of the ZPL line-width was reported [13,171,172]. Major contributions to the T-dependence of the ZPL line-width were identified as resulting from virtual transition into higher confined QD states assisted by LA phonons [173] and, for larger QDs, also real transitions can play a role [174]. As pointed out in Ref [175], for realistic self-assembled QDs both of these mechanisms are insufficient to explain the observed T-dependence quantitatively. Further broadening mechanisms that have been discussed involve acoustic phonon interactions with carriers outside the QD [176] and the finite lifetime of the phonons interacting with the QD [175,177]. The most important intrinsic process limiting the acoustic phonon lifetime is the anharmonic phonon decay [175,178–180]. Further contributions result from phonon scattering by impurities and boundaries [175,177] leading to strongly sample dependent decay rates.

3.2. Non-linear optical signals

The QD-phonon interaction influences also non-linear optical signals like, e.g. pump-probe [111,119] or four-wave-mixing spectra [74,110,111,167,181–183]. As in the linear case, also non-linear spectra comprise a ZPL superimposed on a broad acoustic phonon induced background. The background is non-Lorentzian corresponding to a non-exponential decay in the time-domain. However, the shape of the phonon sideband now strongly depends on parameters like the pulse intensities, the polarizations of the incoming pulses as well as on the pulse delays. In particular, the dependence on the delays can be used to monitor the build-up of the acoustic polaron that forms around the QD position after the optical excitation [111].

Likewise resonance fluorescence spectra comprising a Mollow triplet exhibit significant phonon induced features [184–189]. For example, a temperature-dependent decrease in the Mollow triplet side-band splitting was found, which was attributed to the phonon-renormalization of the driving frequency [190].

A detailed description of the phonon influence on optical QD spectra addressing in particular the Non-Markovian effects can be found in the recent review [191].

4. Resonant nature of carrier-phonon interaction in optical state preparation

Optical state preparation schemes are the backbone of the majority of applications of QDs. However, compared to a discrete energy system without phonons (like an atom) there are fundamental differences that one should be aware of when designing an efficient preparation protocol [24]. In fact, the combined QD phonon dynamics taking place in typical protocols exhibits a number of rather unusual features most of which are related to the resonant nature of the QD-phonon coupling discussed in Sec. 2.2. The phonon influences on the most widely used preparation schemes are the subject of the following subsections.

4.1. Rabi oscillations and rotations

Probably the best known coherent preparation scheme is the excitation with a laser having a fixed central frequency equal to the QD transition frequency resulting in Rabi oscillations [15–17,192–201]. To understand most clearly how Rabi oscillations are affected by effects resulting from the resonant nature of the QD-phonon coupling we consider the case of a continuous excitation switched on instantaneously driving a two-level QD. Without phonons, such an excitation leads to fully modulated undamped Rabi oscillations of the exciton occupation described by a pure sine-function. When coupled to phonons, a damping of the oscillations sets in [15–20] and the stationary value reached by the occupation at long times approaches 0.5 [118,119,151]. This can be well explained in the dressed state picture, where the phonon damping corresponds to a relaxation towards a thermal distribution of the laser-dressed states [119,151,202]. Interestingly, the damping rate depends strongly on the excitation strength, which determines the Rabi frequency of the oscillations [149,150,202]. For a certain Rabi frequency a fast damping occurs, while Rabi frequencies above or below this resonance lead to weaker damping. This behavior is highlighted in Figure 3 (left,top), which shows Rabi oscillations as a function of time for different excitation strengths quantified by the Rabi frequency Ω_R. The strongest damping can be directly connected to the maximum of the phonon spectral density (cf. Figure 1) [16,118].

The dynamics of the exciton system can be well monitored using the Bloch vector defined as $\mathbf{u} = (x, y, z) = (2\mathrm{Re}(p), -2\mathrm{Im}(p), 2f - 1)$ [202,203] defined by the polarization p and the occupation f. For a driven two-level system without phonons, the Bloch vector always moves on the surface of the Bloch sphere and has the length 1. For the Rabi oscillations it describes a circle going from the south pole corresponding to the ground state $|0\rangle$ to the north pole representing the $|x\rangle$ state.
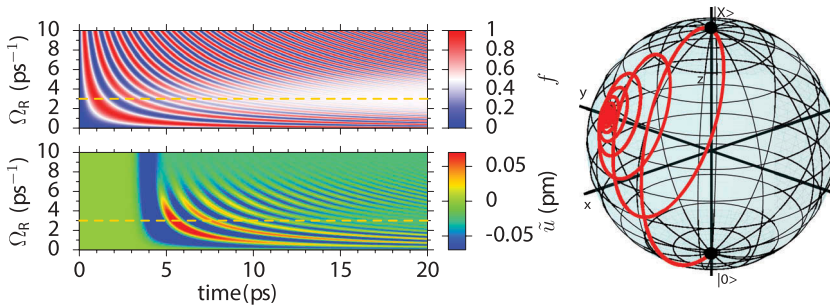
Figure 3. Top: Exciton occupation in a two-level QD coupled to phonons as a function of time and excitation strength for a continuous excitation with the Rabi frequency Ω_R switched on instantaneously at $t = 0$. Bottom: Normalized phonon displacement $\tilde{u}$ at a sphere outside the QD. The dashed lines mark the resonance with the maximum of the phonon spectral density. Results adopted from [118] © IOP Publishing. Right: Dynamics of the Bloch vector on the Bloch sphere for the phonon-damped Rabi oscillations.

With phonons, as shown in Figure 3 (right), the Bloch vector spirals and ends up on the y-axis corresponding to the steady state given by $f = 1/2$ and a finite real polarization p [151].

The damping of the Rabi oscillation is accompanied by the emission of phonon wave packets, which entangles the QD with its environment [204] and, thus, leads to decoherence [93,109,112,167,205]. The formation of the phonon wave packets occurs due to the change of the charge density in the electronic system. When this change happens fast enough, excess energy due to the formation of a polaron is released in form of a phononic wave packet [106]. This is illustrated in Figure 3 (left, bottom) where wave packets at a sphere outside the QD generated by a cw-excitation switched on instantaneously at time $t = 0$ are shown [118]. The amplitude of the wave packets nicely reflects the Rabi oscillations. However, for very large Rabi frequencies, only a single wave packet, which stems from the switch-on process, is emitted, while further wave packet emission is suppressed. Here, the Rabi frequency is well outside the range of the phonon spectral density (cf. Figure 1) and, hence, this is a regime, where the electron and the phonon system are decoupled.

Experimentally it is easier to monitor the final exciton occupation after a short pulse excitation as a function of the pulse area than to record the Rabi oscillations in the time domain. Again an oscillatory behavior emerges, which we denote as *Rabi rotations* in order to distinguish it from the time domain oscillations. In Figure 3 (left, top) Rabi rotations for a rectangular pulse of length τ are found as a vertical cut at $t = \tau$. When going from bottom to top for $t = 20$ ps one starts with unhindered Rabi rotations, followed by a strong damping and then the amplitude of the Rabi rotations again gains in strength. This phenomenon is called

reappearance of Rabi rotations and was predicted more than ten years ago [149,150]. It should be noted that the reappearance is also visible for Gaussian pulses, but there it is less pronounced, because Gaussian pulses contain a spectrum of Rabi frequencies [21]. In most experiments smooth pulses are used and indeed Rabi rotations have been measured up to a pulse area of 12π and clear signs of the phonon damping are visible [19,75]. Although these measurements are in very good agreement with theory, no clear evidence for the reappearance has been found, indicating that the regime of dynamical decoupling of a QD and phonons is hard to reach in Rabi scenarios.

4.2. *Adiabatic rapid passage*

A different method for state preparation is the excitation with chirped laser pulses via the adiabatic rapid passage (ARP) effect [65,207–209]. In a two-level system without phonons, the ARP results in a population inversion which is robust against variations in pulse strength, chirp rate or detuning. The ARP scheme can be used to produce single photons with high indistinguishability [190]. Like for the Rabi rotations, phonons lead to a damping of the ARP effect, but again only for a certain parameter range. At low temperatures, where phonon absorption is suppressed, phonons are only effective for one sign of the chirp, which can be well understood in the dressed state picture [117,138,210,211]. For negative chirp the system is guided along the upper dressed state branch and phonon emission leads to a relaxation towards the lower branch. In contrast, for positive chirp the guidance is along the lower branch, such that phonon induced transitions would require phonon absorption which is, however, inhibited at low temperatures. This asymmetry has been confirmed in several experiments [206,212]. One example for the excitation with chirped pulses is shown in Figure 4 where fluorescence measurements reflecting the exciton occupation after a chirped laser pulse are compared with theoretical predictions. The black curve, which corresponds to almost zero chirp, displays Rabi rotations. The red lines correspond to excitations with positive chirp where a robust population inversion builds up due to the ARP effect as soon as the adiabatic threshold has been overcome. Phonons do not impede this process. The blue curves are results for an excitation with negative chirp. Here the phonons hinder the population inversion and a strong reduction of the ARP effect is visible.

Interestingly, the reduction in Figure 4 exhibits a clear maximum for a pulse area around 3π, while for pulse areas higher than 10π practically no reduction is observed and the curves for positive and negative chirp coincide. Indeed, this proves that at high pulse areas a regime is entered,
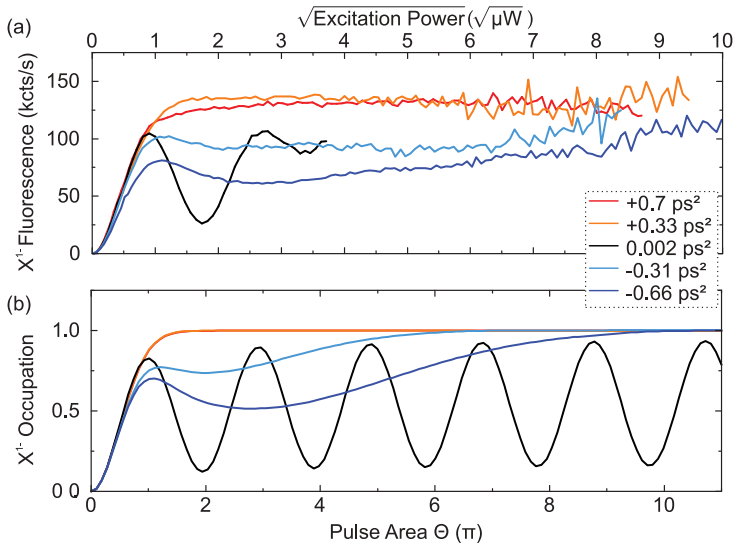
Figure 4. (a) Experimentally measured fluorescence and (b) theoretically calculated occupation corresponding to the excited state of a QD driven by a chirped laser pulse with different chirp rates as indicated. Taken from [206]© American Physical Society.

where electrons and phonons are decoupled exploiting the resonant nature of the carrier-phonon interaction [206]. In this regime the QD dynamics proceeds as if no phonons were present. Because in the ARP effect always a finite splitting between the dressed states exist, it is much easier to enter the decoupling regime than with Rabi rotations, which always scan through all frequencies [93]. Note, that in the decoupling regime, a state preparation which is stable also for elevated temperatures should be possible.

The ARP method can also be applied to prepare the biexciton state in a QD [213–215] where combined carrier-phonon dynamics exhibit similar features like the chirp asymmetry or the dynamic decoupling.
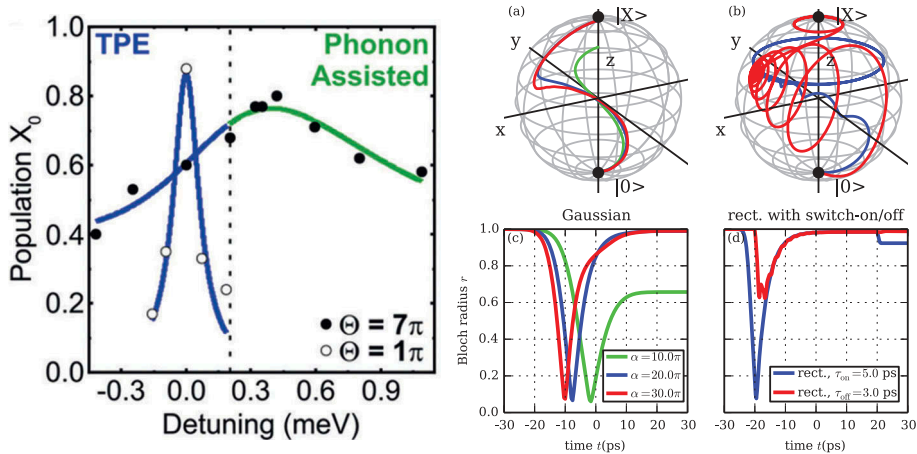
4.3. Phonon-assisted preparation

A pumping directly into the phonon side band can also result in high exciton (or biexciton) occupations [23,25–27,216], which would be impossible without phonons. When a two-level QD is excited with a pulse with a positive detuning from the excitonic transition energy, phonon emission leads to a relaxation into a thermal mixture of the laser-dressed states such that at low temperatures essentially only the lower dressed state is occupied [151]. When driving with a cw laser the exciton occupation at long times is therefore determined by the exciton content of the lower dressed state. The latter approaches one only in the limit of vanishing laser intensity where,

however, the phonon induced relaxation slows down since the phonon coupling between the dressed states is proportional to the exciton content of both dressed states. Thus, with cw driving a perfect phonon-assisted preparation of the exciton is approached asymptotically only at the price of an infinite preparation time [202].

Fortunately, for pulsed excitations, e.g. with Gaussian pulses, a fast phonon-assisted preparation on the timescale of ~10 picoseconds is possible with high fidelity [23,202]. This can be understood by noting that the off-resonant preparation process is actually composed of two separate steps [202]. In a first step phonons lead to a relaxation between laser-dressed states. This is most efficient when the Rabi frequency is tuned to the resonance of the phonon spectral density (cf. Figure 1) and both the initial and the final dressed state have equally large exciton components. The latter condition is always met for strong driving of a two-level system, since for Rabi frequencies much larger than the detuning the probability for being in the exciton state becomes equal for both dressed states and approaches 1/2 (cf., e.g. Equations (9) and (10) in Ref [217].). When the relaxation is completed, the exciton occupation is only about 50% in this scenario since both dressed states have similar exciton components. High exciton occupations are reached in a second step by smoothly switching off the driving laser, which removes the dressing and for positive detuning guides the system adiabatically towards the exciton state [202]. The dynamics of the Bloch vector for the

Figure 5. Left: Phonon-assisted state preparation using two-photon excitation (TPE) for different laser detunings and two excitation strength 1π and 7π. Dots are experimental data, while the solid lines are fits. Taken from [218] under a Creative Commons Attribution. Right: Dynamics of the Bloch vector for phonon-assisted state preparation with (a,b) dynamics of the Bloch sphere and (c,d) length of the Bloch vector for excitation with a Gaussian pulse (a,c) and with a rectangular pulse with either a smooth switch on (blue) or off (red) (b,d). Taken from [202] © American Physical Society.

phonon-assisted state preparation is shown in Figure 5 (right, top) [202]. For the excitation with a Gaussian pulse [see (a,c)] it is interesting to note that the Bloch vector moves through the center of the Bloch sphere, thus, experiences a complete loss and subsequent reappearance of coherence. The two-step character of the preparation is seen best when considering a rectangular pulse with a smoothed edge [see in particular the red curves in (b,d)]. The phonon relaxation in the first step is clearly visible by the spiralling behavior [cf. also Figure 3 (right)] and in the second step during the adiabatic undressing the Bloch vector moves into the north pole of the Bloch sphere.

High fidelity phonon-assisted exciton and biexciton preparation has been demonstrated experimentally in Refs [25,26,218] while selecting the ground state as target can be used for an ultra-fast reset of a QD to its ground state independent of the initial QD occupation [219,220]. Off-resonant phonon-assisted preparation is robust against variations in the pulse intensity or detuning and has the advantage that the exciting laser frequencies are spectrally separated from the QD emission. Unlike other schemes it works better for stronger QD-phonon coupling since it makes active use of the interaction with phonons.

An example for phonon-assisted state preparation is shown in Figure 5 (left), where the QD population is shown as a function of the laser detuning from the two-photon resonance of the ground to biexciton transition for π and 7π pulses. For the π pulse the phonon-induced relaxation between dressed states is rather weak, most likely because the corresponding Rabi frequency is far away from the resonance of the phonon spectral density. As a result, a steep drop of the population is found when the laser is detuned from resonance. In contrast for a 7π pulse a wide plateau is observed, because here phonon-assisted processes become efficient enabling a state preparation for detuned excitations. Even though the state preparation actively uses phonons, no degradation of the quality of subsequently emitted photons in terms of two-photon entanglement and indistinguishability was found [218], indicating that the time-jitter introduced by phonons is of minor importance. A similar result was reported in Ref [26] for the coherence of photons emitted after a phonon-assisted preparation of the biexciton.

The fact, that for the phonon-assisted preparation the resulting population is only weakly affected when the detuning is varied within the range set by the width of the phonon-spectral density (cf. Figure 5) has important practical implications. As demonstrated in Ref [218] it becomes possible to prepare simultaneously two or more QDs in excited states and thus trigger a correlated photon emission from remote QDs. The latter is important for making quantum-information processing protocols scalable.

5. Impact of carrier-phonon interaction on photonic properties

Among the most attractive aspects of QDs are certainly their ability to manipulate properties of photons that interact with them and the possibilities to prepare non-classical photon states such as, e.g. single-photon Fock states or entangled photon pairs. Fock as well as entangled photon states are integral ingredients of innovative developments [221], e.g. in quantum cryptography [222,223], quantum information processing [224–226] and photonics [227]. Furthermore, embedding a QD in a cavity it becomes possible to enter the strong coupling regime, where the quantum states of the QD and the cavity photons are tied together in coherent superpositions. The impact of phonons on these aspects is manifold and pronounced as illustrated by the following examples.

For QD-cavity systems the occurrence of vacuum Rabi oscillations [228–230] and collapse and revival phenomena [231,232] indicate the realization of cavity-QED in the solid state in the strong coupling regime. Phonons coupled to strongly confined QDs lead to a reduction of the vacuum Rabi frequency with rising temperature [154,233,234]. However, even at appreciable temperatures typically no phonon-induced transition from the strong to the weak-coupling regime is found [233,235]. More precisely, if phonon-induced pure dephasing were the only dephasing mechanism vacuum Rabi oscillations should be observed at arbitrarily low QD-cavity couplings λ [154] since by lowering the coupling also the phonon-induced dephasing is reduced. This prevents the system from entering the weak coupling regime where dephasing destroys the coherent energy exchange between QD and cavity. Other relaxation mechanisms, such as those responsible for the broadening of the ZPL, introduce a finite λ value where a transition from strong to weak coupling takes place. The phonon impact on this critical λ value manifests itself in a pronounced dependence on the temperature [154]. For less confined larger QDs a temperature dependent change of the wave function extension of the state from which the emission takes place results in an effectively temperature dependent strength of the dipole coupling, which can overcompensate the reduction of the vacuum Rabi frequency [236].

Another typical strong-coupling feature is the occurence of collapse and revival phenomena [68,237,238]. It turns out that already at zero temperature phonons significantly reduce the amplitude of the revivals [231]. Most remarkable, when increasing the QD-cavity coupling within the range that is typical for current strong-coupling experiments, the revival amplitude counter-intuitively drops with rising coupling strength [231]. Only at very high couplings this trend reverses. Actually, this behavior is another manifestation of the resonant nature of the QD-phonon coupling and can be understood by recalling that the effective phonon-induced damping

depends non-monotonically on the driving strength [150], which in a QD-cavity system is represented by the QD-cavity coupling. Interestingly, in certain parameter regimes, phonons can have a stabilizing effect on the revivals by inhibiting the irregular dynamics that is typical in particular for the atomic Jaynes-Cummings dynamics at low mean photon numbers [232]. Indeed, it has been predicted on the basis of the Jaynes-Cummings model including phonons that even at T = 50 K a sequence of clear revivals can be observed at times where simulations without phonons exhibit a highly irregular time evolution [232].

Much interest has been raised by measurements demonstrating a non-resonant QD-cavity coupling [28,35,36,239–246] of a cavity to an embedded QD, enabling, e.g. to feed photons in a cavity by driving the detuned QD [30]. Photons emitted at frequencies corresponding to the QD and the cavity resonance turn out to be antibunched and anticorrelated [28,36,239,240]. Off-resonant cavity feeding is particularly attractive for applications, since it allows for monitoring the QD dynamics by spectroscopy at the cavity resonance as well as for background free observations of photons emitted from the cavity [28,184,244].

Theoretical studies revealed that phonons provide an efficient coupling mechanism between a QD and a detuned cavity as long as the detuning is not larger than the width of the phonon side-band (i.e. a few meV) [29–34]. Non-resonant QD-cavity coupling has, however, been observed even for detunings of several tens of meV, where the phonon mediated coupling becomes neglibible. Here, shake-up processes in charged QDs [241] and quasicontinuum excitonic transitions involving multi-exciton states [36,246,247] have been discussed as possible origin of the observed effects.

The usability of QDs as single-photon sources has been demonstrated by many groups [48,51,190,248–253] and even triggered as well as deterministic and robust modes of operation of such devices have been reported. Important figures of merit typically used to characterize a single-photon emitter are: the purity, the brightness, the efficiency and the indistinguishability. The purity measures how close a given source comes to the ideal case of releasing exactly one photon in a given emission cycle. It can be determined in coincidence measurements of Hanbury Brown-Twiss type [254], which are related to the conditional probability to detect a second photon when a first one has already been recorded. In this sense purity refers to the suppression of multi-photon emission events. The photon extraction efficiency, which we here refer to as brightness, reflects the average number of photons per excitation pulse extracted from the source [49] while the spontaneous emission (SE) coupling efficiency (also referred to as β-factor) represents the fraction of light emitted into a desired mode, which is most often a cavity mode due to its strong spatial directionality [255]. The indistinguishability quantifies whether or not photons

generated in different excitation cycles are identical. To this end one exploits the fact that when two identical photons arrive simultaneously on the two input channels of a lossless balanced 50:50 beam-splitter, behind the beam splitter the two photons can only be found together in the same output channel while no photons are detected in the other output channel. Of course, which of the two output channels contains the two photons is random and both channels have equal probability. This so called Hong-Ou-Mandel-effect can be monitored by two-photon interference (TPI) measurements [256] and the TPI visibility (corrected by the residual multiphoton probability) is a common measure for the indistinguishability [51]. The theoretical description of the indistinguishability requires the evaluation of second order two-time photon correlation functions [224,255].

5.1. Indistinguishability

In Ref [257] TPI measurements have been performed on photons emitted from a single InGaAs QD. Figure 6(a–c) show TPI coincidence histograms obtained from photons emitted after excitations with a delay $\delta t = 2$ ns for three temperatures T while Figure 6(d) displays the TPI visibility as a function of T. The Hong-Ou-Mandel-effect for ideally identical photons should manifest itself by a vanishing coincidence when the two-photons are not delayed [$\tau = 0$ in Figure 6(a–c)]. Indeed, the counting rate is close to zero at $\tau = 0$ and low temperatures. For higher temperatures it
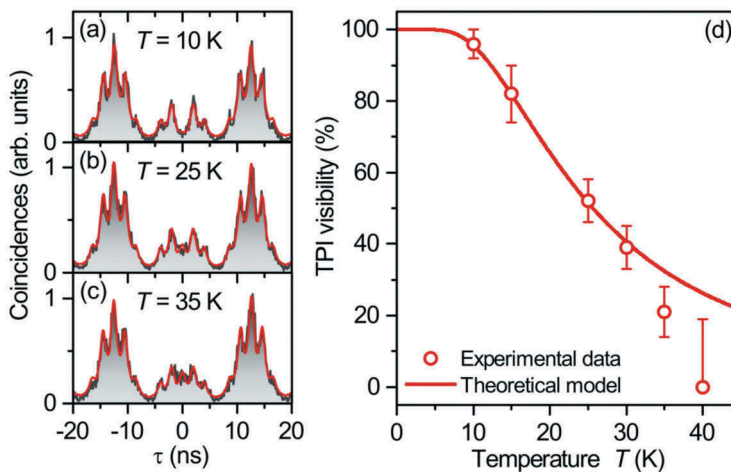
Figure 6. Impact of the temperature on the two-photon interference (TPI) visibility. (a)-(c) TPI histograms for co-polarized configuration at 10, 25, and 35 K and corresponding fits (red solid curves). (d) Experimentally obtained TPI visibilities for various temperatures together with theoretical results accounting for two stochastic forces. Taken from Ref [257].© American Physical Society.

gradually rises indicating a decrease in indistinguishability. Figure 6(d) reveals, that the TPI visibility and thus the indistinguishability falls to zero for temperatures above 40 K. The experimental data in Figure 6(d) has been analyzed by a phenomenological model accounting for two types of stochastic forces representing Gaussian random variables. One force is modeled as white noise and attributed to phonons. The other force is represented as colored noise exhibiting a finite correlation time τ_c. Charge fluctuations have been discussed as possible origin of the colored noise contribution. In this model the TPI visibility is given by:

$$V(\delta t, \tau_c, T) = \frac{\Gamma}{\Gamma'_0(1 - e^{-(\delta t/\tau_c)^2}) + \gamma(T) + \Gamma}, \tag{3}$$

where $\Gamma'_0(1 - e^{-(\delta t/\tau_c)^2})$ stems from the colored noise stochastic force, $\gamma(T)$ is the white noise contribution, while Γ represents the radiative decay rate and δt is the temporal separation between excitations of the QD. Assuming $\gamma(T)$ to arise from the interaction with phonons one expects a proportionality to the square of the mean phonon number [122], i.e. $\gamma(T) = \gamma_0(\bar{n}(T))^2$. In Ref [257] $\bar{n}(T)$ has been parameterized as $\bar{n}(T) = [\exp(\alpha/T) - 1]^{-1}$. Using γ_0 and α as fitting parameters a very good agreement with the experimental results in Figure 6(d) is obtained corroborating the assignment that the reduction of the TPI visibility is indeed due to the interaction with phonons. Thus, phonons completely destroy the indistinguishability of subsequently emitted single photons from a QD when the temperature is above 40 K.

Theoretical studies [255,258] of the phonon impact on the indistinguishability and the efficiency in QD-cavity systems have found pronounced non-Markovian effects. Indeed, comparing results of an exact diagonalization in a strongly reduced phonon state space with a Lindblad-rate treatment as well as with calculations based on a second order time-convolutionless approach revealed strong quantitative and qualitative deviations between exact and approximate results. For example, the Lindblad theory turned out to be unable to capture pronounced asymmetries of the indistinguishability as a function of the detuning between cavity and QD transition frequencies [258], which reflects the asymmetry between phonon absorption and emission.

The crucial influence of phonons on these key figures of merit was further revealed by demonstrating [259] that a cavity-based source cannot simultaneously reach close to unity efficiency and indistinguishability by increasing the cavity Q factor or the QD-cavity coupling strength. The latter was expected on the basis of simple rate models. For explaining this effect it was argued that a QD emits not only in the ZPL but also in phonon sidebands. Due to the different emission frequencies, the emitted photons become more

distinguishable the broader the sideband is. Recalling that a cavity effectively redirects the phonon sideband emission towards the ZPL [cf. Figure 2 (right)] an increase in indistinguishability would be expected. A closer look, however, reveals that the cavity can be considered to act as a filter, removing the phonon-sidebands when the cavity losses are low. The lowering of the SE coupling efficiency caused by the filtering is counter-acted by the Purcell-enhancement of the emission in the zero photon line. All together we are facing a competition of counteracting influences that makes it impossible to reach near unity values of the indistinguishability and the efficiency simultaneously. Recently, it has been shown [133] that accounting for aspects associated with pulsed excitation that can limit simultaneously efficiency and indistinguishability, such as excitation of multiple excitons, multi-photons, and pump-induced dephasing, leads to a further degradation of the source figures of merit which is comparable to the effects caused by phonons. On the other hand, phonons can also have beneficial effects. In particular, a single-photon source with a brightness exceeding 50% has been realized in QD-cavity systems even for QD transition frequencies not matching the cavity frequency [260]. This is possible as long as the QD-cavity detuning is within the range of the phonon sideband since in this case a Purcell enhancement of the emission can take place for phonon-assisted transitions.

5.2. Purity

For practical purposes it is highly desirable to spectrally separate the frequencies of the signal photons from those of the exciting laser pulses to facilitate the monitoring of the signal. To this end one can pump higher energetic dot states and detect photons emitted after a relaxation to lower energetic states. The incoherent nature of the relaxation to the lower state, however, leads to significant uncertainties of the emission times (known as time-jitter) and thus to a loss of control over the emission. Ultra-high purities of photons spectrally separated from the driving laser have been reported using resonant two-photon excitation of the biexciton [261], where, however, the use of a resonant scheme introduces an often unwanted sensitivity on the pulse area and the laser frequency. An alternative is provided by the off-resonant phonon-assisted preparation schemes discussed in Sec. 4.3, which avoid occupations of higher energetic QD states and due to their robustness against variations of pulse area and central laser frequency even allow for scalable preparations of spatially separated QDs emitting coherently [218].

The question whether or not a preparation of QD states relying on the participation of phonons can compete with resonant excitation schemes in terms of the figures of merit of a single-photon source is addressed in Figure 7. Plotted in that figure are purity and brightness as functions of the pulse area for different detunings between the frequencies of the exciting laser and the
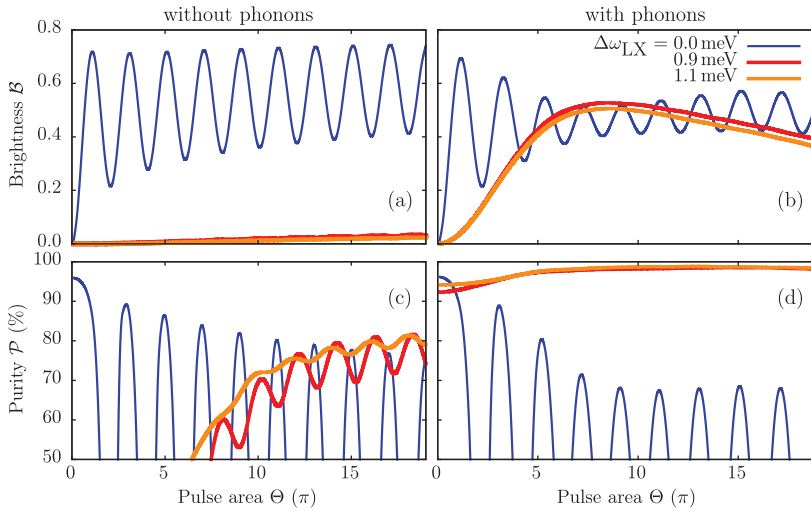
Figure 7. Brightness $\mathcal{B}$ (panels a, b) and single-photon purity $\mathcal{P}$ (panels c, d) as a function of the excitation pulse area θ of a pulse in the pulse train for selected laser-exciton detunings $\Delta\omega_{LX}$. The left column (a, c) is the result of a phonon-free calculation, the right column (b, d) includes the coupling to a continuum of LA phonons. The purity curves have been cut off at the lower end at 50% in order to highlight the behavior at elevated $\mathcal{P}$ values. Results are taken from [288].

QD transition obtained from simulations with (right) and without (left) phonons. Clearly, without phonon assistance the signals for off-resonant excitation are way too low to be of practical use. However, the phonon-induced off-resonant exciton preparation also leads to sizable values of brightness and purity. The maximum value of the purity of 98.8% is even noticeably larger than the maximal achievable value for resonant excitation under otherwise identical conditions, which for the parameters in Figure 7 turns out to be 90.7%. The maximal brightness for off-resonant excitation is reduced compared with the resonant case but is still on an acceptable level. The surprising enhancement of the purity caused by phonons can be explained by recalling (cf. Sec. 4.3) that in an off-resonant preparation process first a relaxation between dressed states takes place, at the end of which the exciton state is typically occupied only to 50%. High exciton occupations are reached subsequently by switching off the driving laser, which removes the dressing and for positive detuning guides the system adiabatically towards the exciton state [202]. The fact that the exciton occupation is built-up not at the pulse maximum but delayed implies that also subsequent processes such as reexcitations of the exciton resulting in the creation of additional photons in the cavity are delayed. This enhances the purity since at the time when the system is returned to the QD ground state with a photon in the cavity, the laser pulse needed for a reexcitation to produce a second photon is already almost gone.

5.3. Entanglement

An application of great practical importance is the use of QDs as sources for (triggered) entangled photon pairs [56,58,262–267]. To this end a QD is usually prepared in the biexciton state $|B\rangle$ and it is exploited that the subsequent decay can proceed along different pathways that eventually return the system to the QD ground state $|G\rangle$ with two photons that are either horizontally (H) or vertically (V) polarized. According to the rules of quantum mechanics the final state will contain in general a coherent superposition of the two two-photon states $|G, HH\rangle$ and $|G, VV\rangle$ which represents a polarization entangled two-photon state. The appearance of entanglement is a genuine quantum mechanical feature which has no classical analog. Maximal entanglement is reached when the superposition is symmetric, which can be achieved only when which-path information is suppressed. In particular, the two excitons that appear as intermediate states of the biexciton decay have to be degenerate and, when the QD is embedded in a cavity, the H and V cavity-photon modes should have the same frequency. Even for degenerate excitons and cavity modes, multi-LO-phonon coupling of the QD to the electronic continuum of wetting layer states can strongly reduce the entanglement for temperatures above 80 K [268]. Under fully symmetric conditions LA phonon-induced pure dephasing has been found to have no impact on the degree of polarization entanglement [269,270] since it affects the two competing pathways in exactly the same way. Indeed, current experiments come close to preparing maximally entangled states either by selecting QDs which naturally have a sufficiently small fine-structure splitting [263,266], by tuning the splitting with external fields [262,271,272], or by applying strain [273]. However, the required effort is rather demanding. In order to achieve high degrees of entanglement even at finite fine-structure splitting δ it has been proposed [274] to place a QD in a cavity and tune the cavity modes in resonance to the two-photon transition between biexciton and ground state. For finite biexciton binding energy of a few meV this set-up strongly favors direct two-photon transitions $|B\rangle \rightarrow |G\rangle$ compared with a sequential single-photon decay of the biexciton first to one of the excitons and then to the ground state. This increases the entanglement by reducing the which-path information caused by the fine-structure splitting, because the direct two-photon process is not much affected by the exciton splitting. Phonons generally reduce the entanglement found for finite δ [62,275,276]. It turns out, however, that for cavity modes in resonance to the two-photon biexciton-ground state transition, the phonon-induced loss of entanglement is much stronger for a finite than for vanishing biexciton binding [276]. This is a result of the frequency dependence of the phonon-spectral density (cf. Figure 1) since the phonon energies needed to compensate for

frequency mismatches are higher for finite than for vanishing biexciton binding energies. For these higher phonon energies the phonon spectral density is higher than for lower ones resulting in an effectively stronger phonon interaction. As a consequence a finite crossing temperature T_{cross} exists above which the configuration with two-photon resonant cavity modes and finite biexciton binding exhibits a lower photon-pair entanglement than in a setting with vanishing biexciton binding. For typical QD parameters T_{cross} is of the order of 10 K or even below [276].

Since the essence of photon-pair entanglement is to maintain a quantum mechanical superposition of different two-photon states with well defined phases between these states and phonons are known to be a major source of decoherence, it was widely believed that phonons can only reduce the entanglement. Surprisingly, a recent study [277] revealed that this is not necessarily true. Under certain circumstances the photon-pair entanglement has been found to be higher with phonons than in the corresponding phonon-free case. In fact, this has been shown to apply to the special situation of either finite exciton or cavity mode splitting and weakly bound biexcitons (typically the biexciton binding energy has to be lower than roughly half the splitting) and occurs for a finite range of QD-cavity coupling strengths. The origin of this phonon-induced enhancement of entanglement is that the loss of coherence caused by phonons can be over-compensated by phonon-induced renormalizations of the QD-cavity coupling that push the system into a regime of higher photon entanglement.

5.4. Photon statistics

Finally, we discuss the phonon impact on QD-cavity systems at elevated mean photon numbers. We concentrate on the special case where the cavity is in the strong coupling limit and the laser driving is comparable with the QD-cavity coupling [37,278], i.e. a regime where there is no obvious small parameter. It turns out that the number of photons in the cavity depends crucially on the excitation conditions. Considering, e.g. a cavity in resonance to the polaron shifted QD transition driven by a cw laser the mean photon number has been determined by path-integral calculations as a function of the laser detuning δ from the QD transition [37]. While at low driving strength the highest photon numbers in the cavity are obtained when the laser is tuned to one of the two cavity split resonances in the linear absorption, there is practically no feature at the corresponding detunings in the strong coupling and driving limit. Instead, the cavity feeding is most efficient when the laser frequency roughly matches transition frequencies between states on the Jaynes-Cummings ladder with adjacent photon numbers near the mean photon number in the cavity. Phonons reduce the peak feeding efficiency.

However, without phonons the feeding efficiency would steeply decrease when the laser is shifted away from the frequency of maximal feeding. Most interestingly, when phonons are accounted for, instead of the steep decrease a wide plateau is found where the feeding efficiency is almost independent of the laser detuning and stays on a rather high value significantly exceeding the phonon-free result [37].

Even more striking is the phonon impact on the stationary photon number distribution reached at long times under strong coupling and driving conditions. Without phonons [cf. Figure 8(a)] one obtains distributions that change qualitatively when varying the laser detuning. Distributions resembling a Poissonian, as expected for a driven empty cavity without an embedded QD, are rarely found in this regime. For some values of δ the distribution even exhibits two distinct maxima. Phonons have a strong qualitative impact on the photon distributions as seen in Figure 8(b). There is still a strong dependence on the detuning, but now the distribution always has a single maximum at zero photon number. Comparing the photon distribution at $\delta = -18\,\mu eV$, i.e. the detuning where the cavity feeding is maximal, with Poissonian and thermal photon distributions of the same mean photon number [cf. Figure 8(c)] reveals that the stationary photon distribution reached in a QD-cavity coupled to phonons at $T = 4$ K is close to a thermal distribution with an effective photon temperature of $T \sim 47{,}000$ K while for a Poissonian distribution the maximum would occur at a finite photon number, which is not observed. Clearly, the phonon impact on the photon statistics is strong and both qualitative and quantitative. Finally, we note that recent advances in measurement techniques made it possible to resolve photon number distributions experimentally by using transition edge sensors [279–282]. Such experiments have already proved their ability to monitor non-classical light emitted from a single QD [282], which justifies the expectation that a wealth of new physical insights concerning the topics discussed in this review will become accessible in the near future.
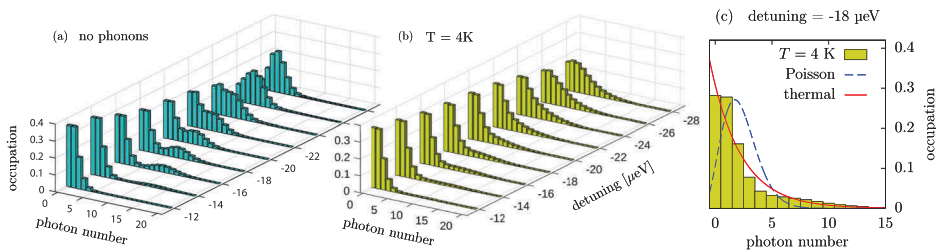
Figure 8. Cavity photon distribution at $t = 3$ ns for different detunings δ and a cavity coupling $\hbar g = 0.1$ meV equal to the laser driving strength. (a) without dot-phonon interaction and (b) with phonons at temperature $T = 4$ K. (c) Photon distribution at detuning $\delta = -18\,\mu eV$ with phonons at $T = 4$ K compared with Poissonian and thermal distributions. Figure taken from [37] © American Physical Society.

6. Conclusions

In this paper, we have reviewed distinctive characteristics of the carrier-phonon interaction in semiconductor quantum dots. Due to the nano-structuring, the carrier-phonon coupling in semiconductor quantum dots has unique features and we discussed their consequences on optical spectra, optical state preparation and the properties of the photons emitted from a quantum dot. Two properties of the carrier-phonon coupling in quantum dots are particularly important: its resonant nature, manifesting itself by a maximum at a finite frequency and a finite frequency range of the coupling, and its super-Ohmic character, which results in pronounced non-Markovian dynamics. A perfect understanding of the physics brought forth by the carrier-phonon interaction will be crucial for their usage in quantum information technology applications, thus, we expect that future research will focus on the role of phonons in these devices. Furthermore, the control and manipulation of the carrier-phonon interaction will become important. To control the phonon properties, one can imagine the usage of phononic cavities [283–285].

Another interesting topic will be the active usage of phonons, which is also referred to as phononics [286,287]. First examples where phonons coupled to semiconductor quantum dots improve application relevant properties include the here discussed phonon-assisted state preparation [23,25–27,218], the establishment of off-resonant QD-cavity couplings [28–36], the phonon mediated brightness enhancement of dots detuned from an embedding cavity [260], the possibility to enhance the photon purity with excitations spectrally separated from the excitation [288], a high cavity-photon feeding efficiency that is robust against variations of the driving frequency [37] as well as the possibility to trigger simultaneous photon emission from remote quantum dots with different transitions frequencies [218]. Further applications comprise lasing manipulated by phonon pulses [289–291], position sensing using phonon shifts [292] or modulations of quantum dots via surface acoustic waves [293–296]. In view of these developments future devices can be expected to benefit from phonons rather than being limited in their functionality.

Disclosure statement

No potential conflict of interest was reported by the authors.

ORCID

D. E. Reiter 🔟 http://orcid.org/0000-0002-3648-353X
T. Kuhn 🔟 http://orcid.org/0000-0001-7449-9287

References

[1] Woggon U. Optical properties of semiconductor quantum dots. Berlin: Springer Verlag; 1997.

[2] Jacak L, Hawrylak P, Wojs A. Quantum dots. Berlin: Springer; 1998.

[3] Michler P (ed). Single quantum dots: Fundamentals, applications and new concepts. Vol. 90. Springer-Verlag Berlin Heidelberg; 2003.

[4] Wang ZM, editor. Self-assembled quantum dots. (Lecture notes in nanoscale science and technology). Vol. 1. New York: Springer; 2008.

[5] Ferreira R, Bastard G. Capture and relaxation in self-assembled semiconductor quantum dots. San Rafael, US-CA: Morgan & Claypool Publishers; 2015.

[6] Bimberg D, Grundmann M, Ledentsov N. Quantum dot heterostructures. Chichester: Wiley; 1999.

[7] Selig M, Berghäuser G, Raja A, et al. Excitonic linewidth and coherence lifetime in monolayer transition metal dichalcogenides. Nat Commun. 2016;7:13279.

[8] Brem S, Selig M, Berghaeuser G, et al. Exciton relaxation cascade in two-dimensional transition metal dichalcogenides. Sci Rep. 2018;8:8238.

[9] Bockelmann U, Bastard G. Phonon scattering and energy relaxation in two-, one-. and zero-dimensional electron gases. Phys Rev B. 1990;42:8947.

[10] Benisty H, Sotomayor-Torres CM, Weisbuch C. Intrinsic mechanism for the poor luminescence properties of quantum-box systems. Phys Rev B. 1991;44:10945.

[11] Heitz R, Born H, Guffarth F, et al. Existence of a phonon bottleneck for excitons in quantum dots. Phys Rev B. 2001;64:241305(R).

[12] Urayama J, Norris TB, Singh J, et al. Observation of phonon bottleneck in quantum dot electronic relaxation. Phys Rev Lett. 2001;86:4930.

[13] Besombes L, Kheng K, Marsal L, et al. Acoustic phonon broadening mechanism in single quantum dot emission. Phys Rev B. 2001;63:155307.

[14] Krummheuer B, Axt VM, Kuhn T. Theory of pure dephasing and the resulting absorption line shape in semiconductor quantum dots. Phys Rev B. 2002;65:195313.

[15] Förstner J, Weber C, Danckwerts J, et al. Phonon-assisted damping of Rabi oscillations in semiconductor quantum dots. Phys Rev Lett. 2003;91:127401.

[16] Machnikowski P, Jacak L. Resonant nature of phonon-induced damping of Rabi oscillations in quantum dots. Phys Rev B. 2004;69:193302.

[17] Krügel A, Axt VM, Kuhn T, et al. The role of acoustic phonons for Rabi oscillations in semiconductor quantum dots. Appl Phys B. 2005;81:897.

[18] Mogilevtsev D, Nisovtsev AP, Kilin S, et al. Non-Markovian damping of Rabi oscillations in semiconductor quantum dots. J Phys Condens Matter. 2009;21:055801.

[19] Ramsay AJ, Gopal AV, Gauger EM, et al. Damping of exciton Rabi rotations by acoustic phonons in optically excited InGaAs/GaAs quantum dots. Phys Rev Lett. 2010;104:17402.

[20] McCutcheon DPS, Dattani NS, Gauger EM, et al. A general approach to quantum dynamics using a variational master equation: application to phonon-damped Rabi rotations in quantum dots. Phys Rev B. 2011;84:081305.

[21] Glässl M, Croitoru MD, Vagov A, et al. Influence of the pulse shape and the dot size on the decay and reappearance of Rabi rotations in laser driven quantum dots. Phys Rev B. 2011;84:125304.

[22] Ramsay AJ. A review of the coherent optical control of the exciton and spin states of semiconductor quantum dots. Semicond Sci Technol. 2010;25:103001.

[23] Glässl M, Barth AM, Axt VM. Proposed robust and high-fidelity preparation of excitons and biexcitons in semiconductor quantum dots making active use of phonons. Phys Rev Lett. 2013;110:147401.

[24] Reiter DE, Kuhn T, Glässl M, et al. The role of phonons for exciton and biexciton generation in an optically driven quantum dot. J Phys Condens Matter. 2014;26 (42):423203.

[25] Ardelt PL, Hanschke L, Fischer KA, et al. Dissipative preparation of the exciton and biexciton in self-assembled quantum dots on picosecond time scales. Phys Rev B. 2014;90:241404.

[26] Bounouar S, Müller M, Barth AM, et al. Phonon-assisted robust and deterministic two-photon biexciton preparation in a quantum dot. Phys Rev B. 2015;91:161302.

[27] Quilter JH, Brash AJ, Liu F, et al. Phonon-assisted population inversion of a single InGaAs/GaAs quantum dot by pulsed laser excitation. Phys Rev Lett. 2015;114:137401.

[28] Ates S, Ulrich SM, Ulhaq A, et al. Non-resonant dot–cavity coupling and its potential for resonant single-quantum-dot spectroscopy. Nat Photon. 2009;3:724.

[29] Naesby A, Suhr T, Kristensen PT, et al. Influence of pure dephasing on emission spectra from single photon sources. Phys Rev A. 2008;78:045802.

[30] Hohenester U, Laucht A, Kaniber M, et al. Phonon-assisted transitions from quantum dot excitons to cavity photons. Phys Rev B. 2009;80:201311.

[31] Hohenester U. Cavity quantum electrodynamics with semiconductor quantum dots: role of phonon-assisted cavity feeding. Phys Rev B. 2010;81:155303.

[32] Majumdar A, Kim E, Gong Y, et al. Phonon mediated off-resonant quantum dot–cavity coupling under resonant excitation of the quantum dot. Phys Rev B. 2011;84:085309.

[33] Hughes S, Yao P, Milde F, et al. Influence of electron-acoustic phonon scattering on off-resonant cavity feeding within a strongly coupled quantum-dot cavity system. Phys Rev B. 2011;83:165313.

[34] Florian M, Gartner P, Gies C, et al. Phonon-mediated off-resonant coupling effects in semiconductor quantum-dot lasers. New J Phys. 2013;15:035019.

[35] Calic M, Gallo P, Felici M, et al. Phonon-mediated coupling of InGaAs/GaAs quantum-dot excitons to photonic crystal cavities. Phys Rev Lett. 2011;106:227402.

[36] Laucht A, Hauke N, Neumann A, et al. Nonresonant feeding of photonic crystal nanocavity modes by quantum dots. J Appl Phys. 2011;109:102404.

[37] Cygorek M, Barth AM, Ungar F, et al. Nonlinear cavity feeding and unconventional photon statistics in solid-state cavity QED revealed by many-level real-time path-integral calculations. Phys Rev B. 2017;96:201201.

[38] Steer MJ, Mowbray DJ, Tribe WR, et al. Electronic energy levels and energy relaxation mechanisms in self-organized InAs/GaAs quantum dots. Phys Rev B. 1996;54:17738.

[39] Heitz R, Veit M, Ledentsov NN, et al. Energy relaxation by multiphonon processes in InAs/GaAs quantum dots. Phys Rev B. 1997;56:10435.

[40] Ignatiev IV, Kozin IE, Davydov VG, et al. Phonon resonances in photoluminescence spectra of self-assembled quantum dots in an electric field. Phys Rev B. 2001;63:075316.

[41] Marcinkevičius S, Gaarder A, Leon R. Rapid carrier relaxation by phonon emission in In$_{0.6}$Ga$_{0.4}$As/GaAs quantum dots. Phys Rev B. 2001;64:115307.

[42] Hameau S, Guldner Y, Verzelen O, et al. Strong electron-phonon coupling regime in quantum dots: evidence for everlasting resonant polarons. Phys Rev Lett. 1999;83:4152.

[43] Hameau S, Isaia JN, Guldner Y, et al. Far-infrared magnetospectroscopy of polaron states in self-assembled InAs/GaAs quantum dots. Phys Rev B. 2002;65:085316.

[44] Verzelen O, Ferreira R, Bastard G. Polaron lifetime and energy relaxation in semiconductor quantum dots. Phys Rev B. 2000;62:R4809.

[45] Jacak L, Krasnyj J, Jacak D, et al. Anharmonicity induced polaron relaxation in GaAs/InAs quantum dots. Phys Rev B. 2002;65:113305.

[46] Jacak L, Krasnyj J, Jacak D, et al. Magneto-polaron in a weakly elliptical InAs/GaAs quantum dot. Phys Rev B. 2003;67:035303.

[47] Zibik EA, Wilson LR, Green RP, et al. Intraband relaxation via polaron decay in InAs self-assembled quantum dots. Phys Rev B. 2004;70:161305(R).

[48] Michler P, Kiraz A, Becher C, et al. A quantum dot single-photon turnstile device. Science. 2000;290:2282.

[49] Gazzano O, Michaelis De Vasconcellos S, Arnold C, et al. Bright solid-state sources of indistinguishable single photons. Nat Commun. 2013;4:1425.

[50] Unsleber S, He YM, Gerhardt S, et al. Highly indistinguishable on-demand resonance fluorescence photons from a deterministic quantum dot micropillar device with 74% extraction efficiency. Opt Express. 2016;24:8539.

[51] Ding X, He Y, Duan ZC, et al. On-demand single photons with high extraction efficiency and near-unity indistinguishability from a resonantly driven quantum dot in a micropillar. Phys Rev Lett. 2016;116:020401.

[52] He YM, Liu J, Maier S, et al. Deterministic implementation of a bright, on-demand single-photon source with near-unity indistinguishability via quantum dot imaging. Optica. 2017;4:802.

[53] Senellart P, Solomon G, White A. High-performance semiconductor quantum-dot single-photon sources. Nat Nanotech. 2017;12:1026.

[54] Müller M, Vural H, Schneider C, et al. Quantum-dot single-photon sources for entanglement enhanced interferometry. Phys Rev Lett. 2017;118:257402.

[55] Reindl M, Weber JH, Huber D, et al. Highly indistinguishable single photons from incoherently and coherently excited GaAs quantum dots. 2019. arXiv:190111251.

[56] Akopian N, Lindner NH, Poem E, et al. Entangled photon pairs from semiconductor quantum dots. Phys Rev Lett. 2006;96:130501.

[57] Winik R, Cogan D, Don Y, et al. On-demand source of maximally entangled photon pairs using the biexciton-exciton radiative cascade. Phys Rev B. 2017;95:235435.

[58] Orieux A, Versteegh MAM, Jöns KD, et al. Semiconductor devices for entangled photon pair generation: a review. Rep Prog Phys. 2017;80:076001.

[59] Chen Y, Zopf M, Keil R, et al. Highly-efficient extraction of entangled photons from quantum dots using a broadband optical antenna. Nat Commun. 2018;9:2994.

[60] Heindel T, Thoma A, von Helversen M, et al. A bright triggered twin-photon source in the solid state. Nat Commun. 2017;8:14870.

[61] Huber D, Reindl M, Huo Y, et al. Highly indistinguishable and strongly entangled photons from symmetric GaAs quantum dots. Nat Commun. 2017;8:15506.

[62] Heinze D, Zrenner A, Schumacher S. Polarization-entangled twin photons from two-photon quantum-dot emission. Phys Rev B. 2017;95:245306.

[63] Huber D, Reindl M, Aberl J, et al. Semiconductor quantum dots as an ideal source of polarization-entangled photon pairs on-demand: a review. J Opt. 2018;20:073002.

[64] Delteil A, Sun Z, Fält S, et al. Realization of a cascaded quantum system: heralded absorption of a single photon qubit by a single-electron charged quantum dot. Phys Rev Lett. 2017;118:177401.

[65] Tannor DJ. Introduction to quantum mechanics. Sausalito, California: University Science Books; 2007.

[66] Jaynes ET, Cummings FW. Comparison of quantum and semiclassical radiation theories with application to the beam maser. Proc IEEE. 1963;51:89.

[67] Shore BW, Knight PL. The Jaynes-Cummings Model. J Mod Opt. 1993;40(7):1195.

[68] Gerry CC, Knight PL. Introductory quantum optics. Cambridge: Cambridge University Press; 2005.

[69] Poem E, Kodriano Y, Tradonsky C, et al. Accessing the dark exciton with light. Nat Phys. 2010;6:993.

[70] Lüker S, Kuhn T, Reiter DE. Direct optical state preparation of the dark exciton in a quantum dot. Phys Rev B. 2015;92:201305.

[71] Lüker S, Kuhn T, Reiter DE. Phonon-assisted dark exciton preparation in a quantum dot. Phys Rev B. 2017;95:195305.

[72] Lüker S, Reiter DE. A review on optical excitation of semiconductor quantum dots under the influence of phonons. Semicond Sci Technol. 2019;34:063002.

[73] Holtkemper M, Reiter DE, Kuhn T. Influence of quantum dot geometry on p-shell transitions in differently charged quantum dots. Phys Rev B. 2018;97:075308.

[74] Vagov A, Axt VM, Kuhn T, et al. Nonmonotonous temperature dependence of the initial decoherence in quantum dots. Phys Rev B. 2004;70:201305.

[75] Ramsay AJ, Godden TM, Boyle SJ, et al. Phonon-induced Rabi-frequency renormalization of optically driven single InGaAs/GaAs quantum dots. Phys Rev Lett. 2010;105:177402.

[76] Krummheuer B, Axt VM, Kuhn T, et al. Pure dephasing and phonon dynamics in GaAs- and GaN-based quantum dot structures: interplay between material parameters and geometry. Phys Rev B. 2005;71:235329.

[77] Ostapenko I, Hönig G, Rodt S, et al. Exciton acoustic-phonon coupling in single GaN/AlN quantum dots. Phys Rev B. 2012;85:081303.

[78] Schuh K, Seebeck J, Lorke M, et al. Rabi oscillations in semiconductor quantum dots revisited: influence of LO-phonon collisions. Appl Phys Lett. 2009;94:201108.

[79] Schuh K, Jahnke F, Lorke M. Rapid adiabatic passage in quantum dots: influence of scattering and dephasing. Appl Phys Lett. 2011;99:011105.

[80] Klimov VI, Ivanov SA, Nanda J, et al. Single-exciton optical gain in semiconductor nanocrystals. Nature. 2007;447:441.

[81] Sauer S, Daniels JM, Reiter DE, et al. Lattice fluctuations at a double phonon frequency with and without squeezing: an exactly solvable model of an optically excited quantum dot. Phys Rev Lett. 2010;105:157401.

[82] Arora AK, Rajalakshmi M, Ravindran TR, et al. Raman spectroscopy of optical phonon confinement in nanostructured materials. J Raman Spectrosc. 2007;38:604.

[83] Woggon U, Gindele F, Wind O, et al. Exchange interaction and phonon confinement in CdSe quantum dots. Phys Rev B. 1996;54:1506.

[84] Fomin VM, Gladilin VN, Devreese JT, et al. Photoluminescence of spherical quantum dots. Phys Rev B. 1998;57:2415.

[85] Yadav HK, Gupta V, Sreenivas K, et al. Low frequency raman scattering from acoustic phonons confined in ZnO nanoparticles. Phys Rev Lett. 2006;97:085502.

[86] Klimov VI, McBranch DW. Femtosecond 1P-to- 1S electron relaxation in strongly confined semiconductor nanocrystals. Phys Rev Lett. 1998;80:4028.

[87] Nandakumar P, Vijayan C, Rajalakshmi M, et al. Raman spectra of CdS nanocrystals in nafion: longitudinal optical and confined acoustic phonon modes. Physica E. 2001;11:377.

[88] Klimov VI, McBranch DW, Leatherdale CA, et al. Electron and hole relaxation pathways in semiconductor quantum dots. Phys Rev B. 1999;60:13740.

[89] Cooney RR, Sewall SL, Anderson KEH, et al. Breaking the phonon bottleneck for holes in semiconductor quantum dots. Phys Rev Lett. 2007;98:177403.

[90] Hyeon-Deuk K, Prezhdo OV. Photoexcited electron and hole dynamics in semiconductor quantum dots: phonon-induced relaxation, dephasing, multiple exciton generation and recombination. J Phys Condens Matter. 2012;24:363201.

[91] Kennehan ER, Doucette GS, Marshall AR, et al. Electron-phonon coupling and resonant relaxation from 1d and 1p states in PbS quantum dots. ACS Nano. 2018;12:6263.

[92] Hartland GV. Coherent excitation of vibrational modes in metallic nanoparticles. Annu Rev Phys Chem. 2006;57:403–430.

[93] Lüker S, Kuhn T, Reiter DE. Phonon impact on optical control schemes of quantum dots: role of quantum dot geometry and symmetry. Phys Rev B. 2017;96:245306.

[94] Munch M, Wüst G, Kuhlmann AV, et al. Manipulation of the nuclear spin ensemble in a quantum dot with chirped magnetic resonance pulses. Nat Nanotech. 2014;9:671.

[95] Nysteen A, Kaer P, Mørk J. Proposed quanching of phonon-induced processes in photoexcited quantum dots due to electron-hole asymmetries. Phys Rev Lett. 2013;110:087401.

[96] Calarco T, Datta A, Fedichev P, et al. Spin-based all-optical quantum computation with quantum dots: understanding and suppressing decoherence. Phys Rev A. 2003;68:012310.

[97] Vagov A, Croitoru M, Glässl M, et al. Real-time path integrals for quantum dots: quantum dissipative dynamics with superohmic environment coupling. Phys Rev B. 2011;83:094303.

[98] Bellingham R, Kent A, Akimov A, et al. Acoustic phonon emission by optically excited carriers in the InAs/GaAs quantum dot system. Phys Status Solidi B. 2001;224:659.

[99] Kent A, Akimov A, Cavill S, et al. Phonon emission by optically pumped indium arsenide quantum dots in gallium arsenide. Physica B. 2002;316–317:198.

[100] Madsen KH, Kaer P, Kreiner-Møller A, et al. Measuring the effective phonon density of states of a quantum dot in cavity quantum electrodynamics. Phys Rev B. 2013;88:045316.

[101] Mahan GD. Many-particle physics. New York: Kluwer; 2000.

[102] Lax M. The Franck-Condon principle and its application to crystals. J Chem Phys. 1950;20:1752.

[103] Huang K, Rhys A. Theory of light absorption and non-radiative transitions in f-centres. Proc R Soc London (A). 1950;204:406.

[104] Roszak K, Machnikowski P. Complete disentanglement by partial pure dephasing. Phys Rev A. 2006;73:022313.

[105] Axt VM, Herbst M, Kuhn T. Coherent control of phonon quantum beats. Superlattices Microstruct. 1999;26:117.

[106] Vagov A, Axt VM, Kuhn T. Electron-phonon dynamics in optically excited quantum dots: exact solution for multiple ultrashort laser pulses. Phys Rev B. 2002;66:165312.

[107] Axt VM, Kuhn T, Vagov A, et al. Phonon-induced pure dephasing in exciton-biexciton quantum dot systems driven by ultrafast laser pulse sequences. Phys Rev B. 2005;72:125309.

[108] Reiter DE, Wigger D, Axt VM, et al. Generation and dynamics of phononic cat states after optical excitation of a quantum dot. Phys Rev B. 2011;84:195327.

[109] Wigger D, Reiter DE, Axt VM, et al. Fluctuation properties of acoustic phonons generated by ultrafast optical excitation of a quantum dot. Phys Rev B. 2013;87:085301.

[110] Vagov A, Axt VM, Kuhn T. Impact of pure dephasing on the nonlinear optical response of single quantum dots and dot ensembles. Phys Rev B. 2003;67:115338.

[111] Krügel A, Vagov A, Axt VM, et al. Monitoring the buildup of the quantum dot polaron: pump-probe and four-wave mixing spectra from excitons and biexcitons in semiconductor quantum dots. Phys Rev B. 2007;76:195302.

[112] Huneke J, Krügel A, Kuhn T, et al. Impact of strain waves traveling across a quantum dot on the optical response of the dot: distinction between strain waves of different origin. Phys Rev B. 2008;78:85316.

[113] Chenu A, Shiau SY, Combescot M. Two-level system coupled to phonons: full analytical solution. Phys Rev B. 2019;99:014302.

[114] Krügel A, Axt VM, Kuhn T. Back action of nonequilibrium phonons on the optically induced dynamics in semiconductor quantum dots. Phys Rev B. 2006;73:035302.

[115] Richter M, Carmele A, Sitek A, et al. Few-photon model of the optical emission of semiconductor quantum dots. Phys Rev Lett. 2009;103:87407.

[116] Vagov A, Croitoru MD, Axt VM, et al. Dynamics of quantum dots with strong electron phonon coupling: correlation expansion vs. path integrals. Phys Status Solidi B. 2011;248:839.

[117] Lüker S, Gawarecki K, Reiter DE, et al. Influence of acoustic phonons on the optical control of quantum dots driven by adiabatic rapid passage. Phys Rev B. 2012;85:121302.

[118] Wigger D, Lüker S, Reiter DE, et al. Energy transport and coherence properties of acoustic phonons generated by optical excitation of a quantum dot. J Phys Condens Matter. 2014;26:255802.

[119] Reiter DE. Time-resolved pump-probe signals of a continuously driven quantum dot affected by phonons. Phys Rev B. 2017;95:125308.

[120] Kubo R. Generalized cumulant expansion method. J Phys Soc Jpn. 1962;17:1100.

[121] Breuer HP, Petruccione F. The theory of open quantum systems. Vol. 28. Oxford: Oxford University Press; 2002.

[122] Carmichael H. Statitical methods in quantum optics 1 - Master Equation and Fokker-Planck equations. Berlin: Springer; 1999.

[123] McCutcheon DPS, Nazir A. Quantum dot Rabi rotations beyond the weak exciton–phonon coupling regime. New J Phys. 2010;12:113042.

[124] Roy C, Hughes S. Influence of electron–acoustic-phonon scattering on intensity power broadening in a coherently driven quantum-dot–cavity system. Phys Rev X. 2011;1:021009.

[125] Kaer P, Nielsen TR, Lodahl P, et al. Microscopic theory of phonon-induced effects on semiconductor quantum dot decay dynamics in cavity QED. Phys Rev B. 2012;86:085302.

[126] Roy C, Hughes S. Polaron master equation theory of the quantum-dot Mollow triplet in a semiconductor cavity-QED system. Phys Rev B. 2012;85:115309.

[127] McCutcheon DPS, Nazir A. Model of the optical emission of a driven semiconductor quantum dot: phonon-enhanced coherent scattering and off-resonant sideband narrowing. Phys Rev Lett. 2013;110:217401.

[128] Hughes S, Carmichael H. Phonon-mediated population inversion in a semiconductor quantum-dot cavity system. New J Phys. 2013;15:053039.

[129] Karwat P, Machnikowski P. Decay and persistence of spatial coherence during phonon-assisted relaxation in double quantum dots. Phys Rev B. 2015;91:125428.

[130] Roy-Choudhury K, Hughes S. Quantum theory of the emission spectrum from quantum dots coupled to structured photonic reservoirs and acoustic phonons. Phys Rev B. 2015;92:205406.

[131] Manson R, Roy-Choudhury K, Hughes S. Polaron master equation theory of pulse-driven phonon-assisted population inversion and single-photon emission from quantum-dot excitons. Phys Rev B. 2016;93:155423.

[132] Nazir A, McCutcheon DPS. Modelling exciton–phonon interactions in optically driven quantum dots. J Phys Condens Matter. 2016;28:103002.

[133] Gustin C, Hughes S. Pulsed excitation dynamics in quantum-dot–cavity systems: limits to optimizing the fidelity of on-demand single-photon sources. Phys Rev B. 2018;98:045309.

[134] Rozbicki E, Machnikowski P. Quantum kinetic theory of phonon-assisted excitation transfer in quantum dot molecules. Phys Rev Lett. 2008;100:27401.

[135] Roszak K, Machnikowski P. Phonon-induced dephasing of singlet-triplet superpositions in double quantum dots without spin-orbit coupling. Phys Rev B. 2009;80:195315.

[136] Roszak K, Machnikowski P. Phonon-induced pure dephasing of two-electron spin states in vertical quantum dot molecules. Acta Phys Pol A. 2009;116:877.

[137] Bagheri Harouni M, Roknizadeh R, Naderi MH. Influence of phonons on exciton-photon interaction and photon statistics of a quantum dot. Phys Rev B. 2009;79:165304.

[138] Gawarecki K, Lüker S, Reiter DE, et al. Dephasing in the adiabatic rapid passage in quantum dots: role of phonon-assisted biexciton generation. Phys Rev B. 2012;86:235301.

[139] Kaer P, Mørk J. Decoherence in semiconductor cavity QED systems due to phonon couplings. Phys Rev B. 2014;90:035312.

[140] Inoshita T, Sakaki H. Density of states and phonon-induced relaxation of electrons in semiconductor quantum dots. Phys Rev B. 1997;56:R4355.

[141] Vasilevskiy MI, Anda EV, Makler SS. Electron-phonon interaction effects in semiconductor quantum dots: a nonperturabative approach. Phys Rev B. 2004;70:035318.

[142] Wilner EY, Wang H, Thoss M, et al. Nonequilibrium quantum systems with electron-phonon interactions: transient dynamics and approach to steady state. Phys Rev B. 2014;89:205129.

[143] Hornecker G, Auffèves A, Grange T. Influence of phonons on solid-state cavity-QED investigated using nonequilibrium Green's functions. Phys Rev B. 2017;95:035404.

[144] Kilina SV, Kilin DS, Prezhdo OV. Breaking the phonon bottleneck in PbSe and CdSe quantum dots: time-domain density functional theory of charge carrier relaxation. ACS Nano. 2009;3:93.

[145] Makri N, Makarov DE. Tensor propagator for iterative quantum time evolution of reduced density matrices. I. Theory. J Chem Phys. 1995;102:4600.

[146] Makri N, Makarov DE. Tensor propagator for iterative quantum time evolution of reduced density matrices. II. Numerical methodology. J Chem Phys. 1995;102:4611.

[147] Liang XT. Non-Markovian dynamics and phonon decoherence of a double quantum dot charge qubit. Phys Rev B. 2005;72:245328.

[148] Thorwart M, Eckel J, Mucciolo ER. Non-Markovian dynamics of double quantum dot charge qubits due to acoustic phonons. Phys Rev B. 2005;72:235320.

[149] Vagov A, Croitoru MD, Axt VM, et al. High pulse area undamping of Rabi oscillations in quantum dots coupled to phonons. Phys Status Solidi B. 2006;243:2233.

[150] Vagov A, Croitoru MD, Axt VM, et al. Nonmonotonic field dependence of damping and reappearance of Rabi oscillations in quantum dots. Phys Rev Lett. 2007;98:227403.

[151] Glässl M, Vagov A, Lüker S, et al. Long-time dynamics and stationary nonequilibrium of an optically driven strongly confined quantum dot coupled to phonons. Phys Rev B. 2011;84:195311.

[152] Glässl M, Croitoru MD, Vagov A, et al. Impact of dark superpositions on the relaxation dynamics of an optically driven phonon-coupled exciton-biexciton quantum-dot system. Phys Rev B. 2012;85:195306.

[153] Glässl M, Axt VM. Polarization dependence of phonon influences in exciton-biexciton quantum dot systems. Phys Rev B. 2012;86:245306.

[154] Vagov A, Glässl M, Croitoru M, et al. Competition between pure dephasing and photon losses in the dynamics of a dot-cavity system. Phys Rev B. 2014;90:075309.

[155] Nahri DG, Mathkoor FHA, Ooi CHR. Real-time path-integral approach for dissipative quantum dot-cavity quantum electrodynamics: impure dephasing-induced effects. J Phys Condens Matter. 2016;29:055701.

[156] Barth AM, Vagov A, Axt VM. Path-integral description of combined Hamiltonian and non-Hamiltonian dynamics in quantum dissipative systems. Phys Rev B. 2016;94:125439.

[157] Strathearn A, Kirton P, Kilda D, et al. Efficient non-Markovian quantum dynamics using time-evolving matrix product operators. Nat Commun. 2018;9:3322.

[158] Feynman RP. Space-time approach to non-relativistic quantum mechanics. Rev Mod Phys. 1948;20:367.

[159] Feynman RP, Vernon F. The theory of a general quantum system interacting with a linear dissipative system. Ann Phys. 1963;24:118.

[160] Cosacchi M, Cygorek M, Ungar F, et al. Path-integral approach for nonequilibrium multitime correlation functions of open quantum systems coupled to Markovian and non-Markovian environments. Phys Rev B. 2018;98:125302.

[161] Guarnieri G, Smirne A, Vacchini B. Quantum regression theorem and non-markovianity of quantum dynamics. Phys Rev A. 2014;90:022110.

[162] McCutcheon DPS. Optical signatures of non-Markovian behavior in open quantum systems. Phys Rev A. 2016;93:022119.

[163] Lodahl P, Mahmoodian S, Stobbe S. Interfacing single photons and single quantum dots with photonic nanostructures. Rev Mod Phys. 2015;87:347.

[164] Favero I, Cassabois G, Ferreira R, et al. Acoustic phonon sidebands in the emission line of single InAs/GaAs quantum dots. Phys Rev B. 2003;68:233301.

[165] Rol F, Founta S, Mariette H, et al. Probing exciton localization in nonpolar GaN/AlN quantum dots by single-dot optical spectroscopy. Phys Rev B. 2007;75:125306.

[166] Stock E, Dachner M, Warming T, et al. Acoustic and optical phonon scattering in a single In(Ga)As quantum dot. Phys Rev B. 2011;83:041304.

[167] Jakubczyk T, Delmonte V, Fischbach S, et al. Impact of phonons on dephasing of individual excitons in deterministic quantum dot microlenses. ACS Photonics. 2016;3:2461.

[168] Grange T, Somaschi N, Antón C, et al. Reducing phonon-induced decoherence in solid-state single-photon sources with cavity quantum electrodynamics. Phys Rev Lett. 2017;118:253602.

[169] Reitzenstein S, Forchel A. Quantum dot micropillars. J Phys D. 2010;43:033001.

[170] Axt VM, Machnikowski P, Kuhn T. Reducing decoherence of the confined exciton state in a quantum dot by pulse-sequence control. Phys Rev B. 2005 Apr;71:155305.

[171] Birkedal D, Leosson K, Hvam JM. Long lived coherence in self-assembled quantum dots. Phys Rev Lett. 2001;87:227401.

[172] Bayer M, Forchel A. Temperature dependence of the exciton homogeneous line-width in $In_{0.60}Ga_{0.40}As/GaAs$ self-assembled quantum dots. Phys Rev B. 2002;65:041308.

[173] Muljarov EA, Zimmermann R. Exciton dephasing in quantum dots due to LO-phonon coupling: an exactly solvable model. Phys Rev Lett. 2007;98:187401.

[174] Takagahara T. Theory of exciton dephasing in semiconductor quantum dots. Phys Rev B. 1999;60:2638.

[175] Rudin S, Reinecke TL, Bayer M. Temperature dependence of optical linewidth in single InAs quantum dots. Phys Rev B. 2006;74:161305(R).

[176] Favero I, Berthelot A, Cassabois G, et al. Temperature dependence of the zero-phonon linewidth in quantum dots: an effect of the fluctuating environment. Phys Rev B. 2007;75:073308.

[177] Ortner G, Yakovlev DR, Bayer M, et al. Temperature dependence of the zero-phonon linewidth in InAsGaAs quantum dots. Phys Rev B. 2004;70:201301(R).

[178] Machnikowski P. Change of decoherence scenario and appearance of localization due to reservoir anharmonicity. Phys Rev Lett. 2006;96:140405.

[179] Machnikowski P. Pure dephasing of carriers in quantum dots due to anharmonicity-induced phonon scattering. Phys Status Solidi B. 2006;243:2247.

[180] Ridley BK. Quantum processes in semiconductors. 5th edition, Oxford University Press, Oxford; 2013.

[181] Borri P, Langbein W, Schneider S, et al. Ultralong dephasing time in InGaAs quantum dots. Phys Rev Lett. 2001;87:157401.

[182] Borri P, Langbein W, Woggon U, et al. Exciton dephasing via phonon interactions in InAs quantum dots: dependence on quantum confinement. Phys Rev B. 2005;71:115328.

[183] Mermillod Q, Wigger D, Delmonte V, et al. Dynamics of excitons in individual InAs quantum dots revealed in four-wave mixing spectroscopy. Optica. 2016;3:377.

[184] Ulhaq A, Ates S, Weiler S, et al. Linewidth broadening and emission saturation of a resonantly excited quantum dot monitored via an off-resonant cavity mode. Phys Rev B. 2010;82:045307.

[185] Ulrich SM, Ates S, Reitzenstein S, et al. Dephasing of triplet-sideband optical emission of a resonantly driven InAs/GaAs quantum dot inside a microcavity. Phys Rev Lett. 2011;106:247402.

[186] Kabuss J, Carmele A, Richter M, et al. Microscopic equation-of-motion approach to the multiphonon assisted quantum emission of a semiconductor quantum dot. Phys Rev B. 2011;84:125324.

[187] Ulhaq A, Weiler S, Roy C, et al. Detuning-dependent Mollow triplet of a coherently-driven single quantum dot. Opt Express. 2013;21:4382.

[188] Wei YJ, He Y, He YM, et al. Temperature-dependent Mollow triplet spectra from a single quantum dot: Rabi frequency renormalization and sideband linewidth insensitivity. Phys Rev Lett. 2014;113:097401.

[189] Morreau A, Muljarov E. Phonon-induced dephasing in quantum dot-cavity QED. arXiv preprint. 2018. arXiv:180710977.

[190] Wei YJ, He YM, Chen MC, et al. Deterministic and robust generation of single photons from a single quantum dot with 99.5% indistinguishability using adiabatic rapid passage. Nano Lett. 2014;14:6515.

[191] Carmele A, Reitzenstein S. Non-markovian features in semiconductor quantum optics: quantifying the role of phonons in experiment and theory. Nanophotonics. 2019;8:655.

[192] Kamada H, Gotoh H, Temmyo J, et al. Exciton Rabi oscillation in a single quantum dot. Phys Rev Lett. 2001;87:246401.

[193] Stievater TH, Li X, Steel DG, et al. Rabi oscillations of excitons in single quantum dots. Phys Rev Lett. 2001;87:133603.

[194] Borri P, Langbein W, Schneider S, et al. Rabi oscillations in the excitonic ground-state transition of InGaAs quantum dots. Phys Rev B. 2002;66:081306.

[195] Htoon H, Takagahara T, Kulik D, et al. Interplay of Rabi oscillations and quantum interference in semiconductor quantum dots. Phys Rev Lett. 2002;88:087401.

[196] Zrenner A, Beham E, Stufler S, et al. Coherent properties of a two-level system based on a quantum-dot photodiode. Nature. 2002;418:612.

[197] Unold T, Mueller K, Lienau C, et al. Optical control of excitons in a pair of quantum dots coupled by the dipole-dipole interaction. Phys Rev Lett. 2005;94:137404.

[198] Danckwerts J, Ahn K, Förstner J, et al. Theory of ultrafast nonlinear optics of Coulomb-coupled semiconductor quantum dots: Rabi oscillations and pump-probe spectra. Phys Rev B. 2006;73:165318.

[199] Stufler S, Machnikowski P, Ester P, et al. Two-photon Rabi oscillations in a single $In_x Ga_{1-x}$ As/GaAs quantum dot. Phys Rev B. 2006;73:125304.

[200] Larson J, Moya-Cessa H. Rabi oscillations in a quantum dot-cavity system coupled to a nonzero temperature phonon bath. Phys Scr. 2008;77:065704.

[201] Schaibley JR, Burgers AP, McCracken GA, et al. Direct detection of time-resolved Rabi oscillations in a single quantum dot via resonance fluorescence. Phys Rev B. 2013;87:115311.

[202] Barth AM, Lüker S, Vagov A, et al. Fast and selective phonon-assisted state preparation of a quantum dot by adiabatic undressing. Phys Rev B. 2016;94:045306.

[203] Allen L, Eberly JH. Optical resonance and two-level atoms. Vol. 28. New York: John Wiley and Sons; 1975.

[204] Machnikowski P, Axt VM, Kuhn T. Quantum-information encoding in dressed qubits. Phys Rev A. 2007;75:052330.

[205] Krummheuer B, Axt VM, Kuhn T. Coupled polarization and acoustic-phonon dynamics after optical excitation of quantum dots near surfaces. Phys Rev B. 2005;72:245336.

[206] Kaldewey T, Lüker S, Kuhlmann AV, et al. Demonstrating the decoupling regime of the electron-phonon interaction in a quantum dot using chirped optical excitation. Phys Rev B. 2017;95:241306.

[207] Schmidgall ER, Eastham PR, Phillips RT. Population inversion in quantum dot ensembles via adiabatic rapid passage. Phys Rev B. 2010;81:195306.

[208] Simon CM, Belhadj T, Chatel B, et al. Robust quantum dot exciton generation via adiabatic passage with frequency-swept optical pulses. Phys Rev Lett. 2011;106:166801.

[209] Wu Y, Piper IM, Ediger M, et al. Population inversion in a single InGaAs quantum dot using the method of adiabatic rapid passage. Phys Rev Lett. 2011;106:067401.

[210] Debnath A, Meier C, Chatel B, et al. Chirped laser excitation of quantum dot excitons coupled to a phonon bath. Phys Rev B. 2012;86:161304.

[211] Eastham PR, Spracklen AO, Keeling J. Lindblad theory of dynamical decoherence of quantum-dot excitons. Phys Rev B. 2013;87:195306.

[212] Mathew R, Dilcher E, Gamouras A, et al. Subpicosecond adiabatic rapid passage on a single semiconductor quantum dot: phonon-mediated dephasing in the strong-driving regime. Phys Rev B. 2014;90:035316.

[213] Glässl M, Barth AM, Gawarecki K, et al. Biexciton state preparation in a quantum dot via adiabatic rapid passage: comparison between two control protocols and impact of phonon-induced dephasing. Phys Rev B. 2013;87:085303.

[214] Debnath A, Meier C, Chatel B, et al. High-fidelity biexciton generation in quantum dots by chirped laser pulses. Phys Rev B. 2013;88:201305.

[215] Kaldewey T, Lüker S, Kuhlmann AV, et al. Coherent and robust high-fidelity generation of a biexciton in a quantum dot with rapid adiabatic passage. Phys Rev B. 2017;95:161302.

[216] Reiter DE, Lüker S, Gawarecki K, et al. Phonon effects on population inversion in quantum dots: resonant, detuned and frequency-swept excitations. Acta Phys Pol A. 2012;122:1065.

[217] Vitanov NV, Halfmann T, Shore BW, et al. Laser-induced population transfer by adiabatic passage techniques. Annu Rev Phys Chem. 2001;52(1):763–809. PMID: 11326080.

[218] Reindl M, Jons KD, Huber D, et al. Phonon-assisted two-photon interference from remote quantum emitters. Nano Lett. 2017;17:4090.

[219] Liu F, Martins LMP, Brash AJ, et al. Ultrafast depopulation of a quantum dot by LA-phonon-assisted stimulated emission. Phys Rev B. 2016;93:161407.

[220] Brash AJ, Martins LMPP, Barth AM, et al. Dynamic vibronic coupling in InGaAs quantum dots. J Opt Soc Am B. 2016;33:C115.

[221] Zeilinger A. Light for the quantum. entangled photons and their applications: a very personal perspective. Phys Scr. 2017;92:072501.

[222] Stevenson RM, Thompson RM, Shields AJ, et al. Quantum dots as a photon source for passive quantum key encoding. Phys Rev B. 2002;66:081302.

[223] Gisin N, Ribordy G, Tittel W, et al. Quantum cryptography. Rev Mod Phys. 2002;74:145.

[224] Kiraz A, Atatüre M, Imamoğlu A. Quantum-dot single-photon sources: prospects for applications in linear optics quantum-information processing. Phys Rev A. 2004;69:032305.

[225] Pan JW, Chen ZB, Lu CY, et al. Multiphoton entanglement and interferometry. Rev Mod Phys. 2012;84:777.

[226] Kuhn SC, Knorr A, Reitzenstein S, et al. Cavity assisted emission of single, paired and heralded photons from a single quantum dot device. Opt Express. 2016;24:25446.

[227] O'Brian JL, Furusawa A, Vučković J. Photonic quantum technologies. Nat Photon. 2009;3:687.

[228] Reithmaier JP, Sek G, Löffler A, et al. Strong coupling in a single quantum dot–semiconductor microcavity system. Nature. 2004;432:197.

[229] Yoshie T, Scherer A, Hendrickson J, et al. Vacuum Rabi splitting with a single quantum dot in a photonic crystal nanocavity. Nature. 2004;432:200.

[230] Khitrova G, Gibbs HM, Kira M, et al. Vacuum Rabi splitting in semiconductors. Nat Phys. 2006;2:81.

[231] Glässl M, Sörgel L, Vagov A, et al. Interaction of a quantum-dot cavity system with acoustic phonons: stronger light-matter coupling can reduce the visibility of strong coupling effects. Phys Rev B. 2012;86:035319.

[232] Carmele A, Knorr A, Milde F. Stabilization of photon collapse and revival dynamics by a non-Markovian phonon bath. New J Phys. 2013;15:105024.

[233] Wilson-Rae I, Imamoğlu A. Quantum dot cavity-QED in the presence of strong electron-phonon interactions. Phys Rev B. 2002;65:235311.

[234] Laucht A, Hauke N, Villas-Bôas JM, et al. Dephasing of exciton polaritons in photoexcited ingaas quantum dots in gaas nanocavities. Phys Rev Lett. 2009;103:087405.

[235] Milde F, Knorr A, Hughes S. Role of electron-phonon scattering on the vacuum Rabi splitting of a single-quantum dot and a photonic crystal nanocavity. Phys Rev B. 2008;78:035330.

[236] Hopfmann C, Musiał A, Strauß M, et al. Compensation of phonon-induced renormalization of vacuum Rabi splitting in large quantum dots: towards temperature-stable strong coupling in the solid state with quantum dot-micropillars. Phys Rev B. 2015;92:245403.

[237] Eberly JH, Narozhny NB, Sanchez-Mondragon JJ. Periodic spontaneous collapse and revival in a simple quantum model. Phys Rev Lett. 1980;44:1323.

[238] Rempe G, Walther H, Klein N. Observation of quantum collapse and revival in a one-atom maser. Phys Rev Lett. 1987;58:353.

[239] Hennessy K, Badolato A, Winger M, et al. Quantum nature of a strongly coupled single quantum dot-cavity system. Nature. 2007;445:896.

[240] Press D, Götzinger S, Reitzenstein S, et al. Photon antibunching from a single quantum-dot-microcavity system in the strong coupling regime. Phys Rev Lett. 2007;98:117402.

[241] Kaniber M, Laucht A, Neumann A, et al. Investigation of the nonresonant dot-cavity coupling in two-dimensional photonic crystal nanocavities. Phys Rev B. 2008;77:161303.

[242] Laucht A, Hofbauer F, Hauke N, et al. Electrical control of spontaneous emission and strong coupling for a single quantum dot. New J Phys. 2009;11:023034.

[243] Suffczyński J, Dousse A, Gauthron K, et al. Origin of the optical emission within the cavity mode of coupled quantum dot-cavity systems. Phys Rev Lett. 2009;103:027401.

[244] Englund D, Majumdar A, Faraon A, et al. Resonant excitation of a quantum dot strongly coupled to a photonic crystal nanocavity. Phys Rev Lett. 2010;104:073904.

[245] Dalacu D, Mnaymneh K, Sazonova V, et al. Deterministic emitter-cavity coupling using a single-site controlled quantum dot. Phys Rev B. 2010;82:033301.

[246] Laucht A, Kaniber M, Mohtashami A, et al. Temporal monitoring of nonresonant feeding of semiconductor nanocavity modes by quantum dot multiexciton transitions. Phys Rev B. 2010;81:241302.

[247] Winger M, Volz T, Tarel G, et al. Explanation of photon correlations in the far-off-resonance optical emission from a quantum-dot–cavity system. Phys Rev Lett. 2009;103:207403.

[248] Santori C, Pelton M, Solomon G, et al. Triggered single photons from a quantum dot. Phys Rev Lett. 2001;86:1502.

[249] Santori C, Fattal D, Vučković J, et al. Indistinguishable photons from a single-photon device. Nature. 2002;419:594.

[250] He YM, He Y, Wei YJ, et al. On-demand semiconductor single-photon source with near-unity indistinguishability. Nat Nanotech. 2013;8:213.

[251] Somaschi N, Giesz V, De Santis L, et al. Near-optimal single-photon sources in the solid state. Nat Photon. 2016;10:340.

[252] Schweickert L, Jöns KD, Zeuner KD, et al. On-demand generation of background-free single photons from a solid-state source. Appl Phys Lett. 2018;112:093106.

[253] Schlehahn A, Fischbach S, Schmidt R, et al. A stand-alone fiber-coupled single-photon source. Sci Rep. 2018;8:1340.

[254] Hanbury Brown R, Twiss RQ. A test of a new type of stellar interferometer on Sirius. Nature. 1956;178:1046.

[255] Kaer P, Gregersen N, Mork J. The role of phonon scattering in the indistinguishability of photons emitted from semiconductor cavity QED systems. New J Phys. 2013;15:035027.

[256] Hong CK, Ou ZY, Mandel L. Measurement of subpicosecond time intervals between two photons by interference. Phys Rev Lett. 1987;59:2044.

[257] Thoma A, Schnauber P, Gschrey M, et al. Exploring dephasing of a solid-state quantum emitter via time-and temperature-dependent Hong-Ou-Mandel experiments. Phys Rev Lett. 2016;116:033601.

[258] Kaer P, Lodahl P, Jauho AP, et al. Microscopic theory of indistinguishable single-photon emission from a quantum dot coupled to a cavity: the role of non-Markovian phonon-induced decoherence. Phys Rev B. 2013;87:081308.

[259] Iles-Smith J, McCutcheon DPS, Nazir A, et al. Phonon scattering inhibits simultaneous near-unity efficiency and indistinguishability in semiconductor single-photon sources. Nat Photon. 2017;11:521.

[260] Portalupi SL, Hornecker G, Giesz V, et al. Bright phonon-tuned single-photon source. Nano Lett. 2015;15:6290.

[261] Hanschke L, Fischer KA, Appel S, et al. Quantum dot single-photon sources with ultra-low multi-photon probability. Npj Quantum Inf. 2018;4:43.

[262] Stevenson RM, Young RJ, Atkinson P, et al. A semiconductor source of triggered entangled photon pairs. Nature. 2006;439:179.

[263] Hafenbrak R, Ulrich SM, Michler P, et al. Triggered polarization-entangled photon pairs from a single quantum dot up to 30K. New J Phys. 2007;9:315.

[264] Dousse A, Suffczyński J, Beveratos A, et al. Ultrabright source of entangled photon pairs. Nature. 2010;466:217.

[265] Del Valle E. Distilling one, two and entangled pairs of photons from a quantum dot with cavity QED effects and spectral filtering. New J Phys. 2013;15:025019.

[266] Müller M, Bounouar S, Jöns KD, et al. On-demand generation of indistinguishable polarization-entangled photon pairs. Nat Photon. 2014;8:224.

[267] Sánchez Muñoz C, Laussy FP, Tejedor C, et al. Enhanced two-photon emission from a dressed biexciton. New J Phys. 2015;17:123021.

[268] Carmele A, Milde F, Dachner MR, et al. Formation dynamics of an entangled photon pair: a temperature-dependent analysis. Phys Rev B. 2010;81:195319.

[269] Carmele A, Knorr A. Analytical solution of the quantum-state tomography of the biexciton cascade in semiconductor quantum dots: pure dephasing does not affect entanglement. Phys Rev B. 2011;84:075328.

[270] Cygorek M, Ungar F, Seidelmann T, et al. Comparison of different concurrences characterizing photon pairs generated in the biexciton cascade in quantum dots coupled to microcavities. Phys Rev B. 2018;98:045303.

[271] Young RJ, Stevenson RM, Atkinson P, et al. Improved fidelity of triggered entangled photons from single quantum dots. New J Phys. 2006;8:29.

[272] Stevenson RM, Young RJ, See P, et al. Magnetic-field-induced reduction of the exciton polarization splitting in InAs quantum dots. Phys Rev B. 2006;73:033306.

[273] Zhang J, Wildmann JS, Ding F, et al. High yield and ultrafast sources of electrically triggered entangled-photon pairs based on strain-tunable quantum dots. Nat Commun. 2015;6:10067.

[274] Schumacher S, Förstner J, Zrenner A, et al. Cavity-assisted emission of polarization-entangled photons from biexcitons in quantum dots with fine-structure splitting. Opt Express. 2012;20:5335.

[275] Harouni MB. Phonon-induced effects on exciton dynamics and photon emission from a semiconductor quantum dot microcavity: phonon coherent state representation. Laser Phys. 2014;24:045201.

[276] Seidelmann T, Ungar F, Cygorek M, et al. From strong to weak temperature dependence of the two-photon entanglement resulting from the biexciton cascade inside a cavity. Phys Rev B. 2019;99:245301.

[277] Seidelmann T, Ungar F, Barth AM, et al. Phonon-induced enhancement of photon entanglement in quantum dot-cavity systems. 2019. arXiv:190204933.

[278] Hopfmann C, Carmele A, Musiał A, et al. Transition from Jaynes-Cummings to Autler-Townes ladder in a quantum dot–microcavity system. Phys Rev B. 2017;95:035302.

[279] Schmidt M, von Helversen M, López M, et al. Photon-number-resolving transition-edge sensors for the metrology of quantum light sources. J Low Temp Phys. 2018;193(5):1243.

[280] Klaas M, Schlottmann E, Flayac H, et al. Photon-number-resolved measurement of an exciton-polariton condensate. Phys Rev Lett. 2018;121:047401.

[281] Schlottmann E, von Helversen M, Leymann HAM, et al. Exploring the photon-number distribution of bimodal microlasers with a transition edge sensor. Phys Rev Appl. 2018;9:064030.

[282] van Helversen M, Böhm J, Schmidt M, et al. Quantum metrology of solid-state single-photon sources using photon-number-resolving detectors. New J Phys. 2019;21:035007.

[283] Lanzillotti-Kimura N, Fainstein A, Balseiro C, et al. Phonon engineering with acoustic nanocavities: theoretical considerations on phonon molecules, band structures, and acoustic Bloch oscillations. Phys Rev B. 2007;75:024301.

[284] Kabuss J, Carmele A, Brandes T, et al. Optically driven quantum dots as source of coherent cavity phonons: a proposal for a phonon laser scheme. Phys Rev Lett. 2012;109:054301.

[285] Esmann M, Lamberti FR, Senellart P, et al. Topological nanophononic states by band inversion. Phys Rev B. 2018;97:155422.

[286] Kerfoot ML, Govorov AO, Czarnocki C, et al. Optophononics with coupled quantum dots. Nat Commun. 2014;5:3299.

[287] Volz S, Ordonez-Miranda J, Shchepetov A, et al. Nanophononics: state of the art and perspectives. Eur Phys J B. 2016;89:1.

[288] Cosacchi M, Ungar F, Cygorek M, et al. Emission-frequency separated high quality single-photon sources enabled by phonons. Phys Rev Lett. 2019;123:017403.

[289] Brüggemann C, Akimov AV, Scherbakov AV, et al. Laser mode feeding by shaking quantum dots in a planar microcavity. Nat Photon. 2011;6:30.

[290] Czerniuk T, Wigger D, Akimov AV, et al. Picosecond control of quantum dot laser emission by coherent phonons. Phys Rev Lett. 2017;118:133901.

[291] Wigger D, Czerniuk T, Reiter DE, et al. Systematic study of the influence of coherent phonon wave packets on the lasing properties of a quantum dot ensemble. New J Phys. 2017;19:073001.

[292] Fons R, Osterkryger AD, Stepanov P, et al. All-optical mapping of the position of quantum dots embedded in a nanowire antenna. Nano Lett. 2018;18:6434.

[293] Kataoka M, Schneble RJ, Thorn AL, et al. Single-electron population and depopulation of an isolated quantum dot using a surface-acoustic-wave pulse. Phys Rev Lett. 2007;98:046801.

[294] Gell JR, Ward MB, Young RJ, et al. Modulation of single quantum dot energy levels by a surface-acoustic-wave. Appl Phys Lett. 2008;93:081115.

[295] Blattmann R, Krenner HJ, Kohler S, et al. Entanglement creation in a quantum-dot–nanocavity system by Fourier-synthesized acoustic pulses. Phys Rev A. 2014;89:012327.

[296] Weiß M, Hörner AL, Zallo E, et al. Multiharmonic frequency-chirped transducers for surface-acoustic-wave optomechanics. Phys Rev Appl. 2018;9:014004.